Original Article

MOLECULAR METABOLISM

Training-induced plasma miR-29a-3p is secreted by skeletal muscle and contributes to metabolic adaptations to resistance exercise in mice

Paola Pinto-Hernandez[1,2,12], Manuel Fernandez-Sanjurjo[1,2,,12], Daan Paget[3], Xurde M. Caravia[4,5], David Roiz-Valle[6], Juan Castilla-Silgado[1,2], Sergio Diez-Robles[1], Almudena Coto-Vilcapoma[1], David Fernandez-Vivero[1,2], Pau Gama-Perez[7], Pablo M. Garcia-Roves[8,9], Carlos Lopez-Otin[6], Juleen R. Zierath[3,10], Anna Krook[3], Benjamin Fernandez-Garcia[2,11,13], Cristina Tomas-Zapico[1,2,13], Eduardo Iglesias-Gutierrez[1,2,*,13]**

ABSTRACT

Objective: The adaptive response to different models of regular exercise involves complex tissue crosstalk. Our aim was to explore the involvement of extracellular vesicle (EV) microRNAs (miRNAs) in this process, the secretory role of skeletal muscle and its functional metabolic interaction with the liver.

Methods: Plasma EV miRNAs obtained from mice after 4-weeks of endurance or resistance training were sequenced. Subsequent experiments using trained genetically modified mouse models and in vitro approaches involving knock-down and electrostimulated cells, were conducted.

Results: Resistance training increased the expression of a group of 11 miRNAs functionally divided into two clusters. Among them, miR-29a-3p emerges as a molecular mediator released in EVs by skeletal muscle, with a relevant role in adaptation to endurance training, by contributing to modulate the expression and secretion of other miRNAs associated with training and regulating processes related to substrate availability, transport, and metabolic use in skeletal muscle and liver.

Conclusions: Our study suggests that miR-29a-3p is a training-induced molecular mediator in the response and adaptation to resistance training, possibly due to its regulatory role in energy metabolism in skeletal muscle in response to exercise.

Keywords microRNAs; Exercise training; miR-29 family; Extracellular vesicles; Energy metabolism

1. INTRODUCTION

The benefits of regular exercise for improving quality of life, as well as for the prevention and/or adjuvant treatment of chronic diseases, have been widely demonstrated [1]. The systemic response to exercise involves not only skeletal muscle, as the primary responder to this stimulus, but also different tissues, including liver, heart, adipose tissue, kidneys, skin, pancreas, or brain [2]. However, the molecular

[1]Department of Functional Biology, Area of Physiology, University of Oviedo, Oviedo, Asturias, 33006, Spain [2]Health Research Institute of the Principality of Asturias (ISPA), Oviedo, Asturias, 33011, Spain [3]Department of Physiology and Pharmacology, Karolinska Institutet, Stockholm, Sweden [4]Department of Molecular Biology, University of Texas Southwestern Medical Center, Dallas, TX, 75390, USA [5]Hamon Center for Regenerative Science and Medicine, University of Texas Southwestern Medical Center, Dallas, TX, 75390, USA [6]Department of Biochemistry and Molecular Biology. University Institute of Oncology, University of Oviedo, Oviedo, Asturias, 33006, Spain [7]Department of Physiological Sciences II, Faculty of Medicine-University of Barcelona, Hospitalet del Llobregat, Barcelona, Spain [8]University of Barcelona, Barcelona, Spain [9]Institut d'Investigació Biomèdica de Bellvitge (IDIBELL), L'Hospitalet de Llobregat, Barcelona, Spain [10]Department of Molecular Medicine and Surgery, Karolinska Institutet, Stockholm, Sweden [11]Department of Morphology and Cell Biology, Anatomy, University of Oviedo, Oviedo, 33006, Spain

[12] Pinto-Hernandez, Paola and Fernandez-Sanjurjo, Manuel contributed equally to this work as first authors.

[13] These authors contributed equally to this work as last authors.

*Corresponding author. Department of Functional Biology (Physiology), University of Oviedo, Avda. Julián Clavería 6, Oviedo, Asturias, 33006, Spain. E-mail: iglesiaseduardo@uniovi.es (E. Iglesias-Gutierrez).

**Corresponding author. Health Research Institute of the Principality of Asturias (ISPA), Oviedo, Asturias, 33011, Spain. E-mail: manufsanjurjo@gmail.com (M. Fernandez-Sanjurjo).

Abbreviations: END, Endurance; EPS, Electrical pulse stimulation; EVs, Extracellular vesicles; Fbp1, Fructose-1,6-bisphosphatase 1; FC, Fold change; miR-29KO, *miR-29a/b1* cluster knock-out; miR-29KOCON, MiR-29KO sedentary mice; miR-29KOEND, Endurance-trained miR-29KO mice; miR-29KORES, Resistance-trained miR-29KO mice; miRNAs, microRNAs; myomiRs, skeletal muscle-associated miRNAs; NGS, Short RNA next generation sequencing; Pfkm, Phosphofructo-1-kinase; RES, Resistance; RPM, Reads Per Million; TPM, Transcripts Per Kilobase Million

Received May 16, 2025 • Accepted May 20, 2025 • Available online 23 May 2025

https://doi.org/10.1016/j.molmet.2025.102173

adaptations underlying this finely orchestrated multisystemic response, mediated by an intense inter-tissue crosstalk, have not been fully explored.

Several authors have reported the release of extracellular vesicles (EVs) into the systemic circulation from different tissues and blood cell types, that may participate in cell communication signaling during the response and adaptation to exercise [3]. Thus, Whitham et al. [4] described intercellular interactions between skeletal muscle and liver, mediated by protein transport via EV trafficking, in response to an acute bout of endurance exercise. Interestingly, EVs internalization by recipient cells implies the ability of their cargo to modify and/or induce different physiological pathways [5,6]. As reviewed by Estébanez et al. [7] and Darragh et al. [8], changes not only in EV abundance but also in cargo profile has been described in response to acute exercise of different modalities and at rest in trained individuals, both in rodents and humans. Apart from proteins, the EV cargo comprises a variety of other macromolecules, including microRNAs (miRNAs) [9]. MiRNAs are small non-coding RNA molecules ($\approx$22 nucleotides) with a post-transcriptional gene expression regulatory function, by promoting mRNA degradation or by repressing protein translation [10]. Therefore, miRNAs contained in EVs may modulate the gene expression and phenotype of distant recipient cells [11]. Skeletal muscle acts as an important endocrine organ and it may also have the capacity to release miRNA-loaded EVs into the systemic circulation during exercise [12], while the liver has been described as the main recipient of plasma EVs [4]. Therefore, it is worth considering whether the adaptive response to different models of regular exercise is, at least in part, mediated by EV miRNAs released by skeletal muscle and its functional metabolic interaction with liver.

In this study, we report the analysis of miRNA-loaded plasma EVs obtained from mice after 4-weeks of endurance or resistance training. We found that resistance exercise exerts a higher and significant change in this profile. Using in silico approaches, we determined that these EV miRNAs are mainly organized in two functional clusters. Based on these data and using both genetically modified murine models and cellular *in vitro* approaches, we explored the role of miR-29a-3p as a molecular mediator released in EVs by contracting skeletal muscle, appearing to play a role in the adaptation to resistance training through its regulatory role in energy metabolism pathways, both in skeletal muscle and liver.

2. MATERIALS AND METHODS

2.1. Mice

30 male mice of the C57BL/6N genetic background (Wild-type; WT) were obtained from Charles River Laboratories. Parental male and female *miR-29a/b1* heterozygous (*miR-29a/b1*$^{+/-}$) mice on C57BL/6N genetic background were kindly provided by Dr. Carlos Otín's research group [13], from which *miR-29a/b1*$^{-/-}$ mice were generated (miR-29KO).

A total of 26, 10-week-old, WT male mice and 23, 10-week-old, miR-29KO male mice were randomly divided into three different groups: sedentary control (CON, $n = 6$; miR-29KOCON, $n = 8$), endurance training (END, $n = 12$; miR-29KOEND, $n = 7$) and resistance training (RES, $n = 8$; miR-29KORES, $n = 8$). Additionally, 16-week-old WT ($n = 4$) and miR-29KO ($n = 4$) mice were used to perform a maximal endurance performance test to determine blood glucose and lactate threshold levels.

Mice were fed using a pellet rodent diet (Teklad Irradiated Global 18% Protein Rodent Diet, Envigo, Spain) and water *ad libitum*. Food intake and body mass were recorded on a weekly basis (Fig. S1). Mice were maintained on a 12 h light/dark cycle (light onset at 8:00 AM) and under controlled temperature (22 $\pm$ 2 °C) at the Animal Facilities of the University of Oviedo, Spain (authorized facility No. ES330440003591).

All procedures were conducted during the early light portion of the cycle and performed in accordance with the institutional guidelines approved by The Research Ethics Committee of the University of Oviedo, Spain (PROAE 10/2016 and PROAE 35/2020).

2.2. Exercise interventions

A 4-week endurance or resistance training intervention for WT and miR-29KO was applied. Endurance training was conducted on a commercial four-rail treadmill (TSE Systems, Germany) with adjustable speed and incline, without any aversive stimuli. Resistance training was carried out using a previously described own-manufactured static ladder [14]. The same researcher handled and trained the mice during the different stages of the exercise intervention: acclimation period, specific maximal performance tests (pre- and post-training), and training protocols, as well as the lactate threshold test.

2.2.1. Acclimation period

Mice were acclimatized to the training devices for 2 weeks, 5 sessions per week, and 15 min per training session, as previously described [15,16].

2.2.2. Maximal performance tests

Twenty-four hours after the end of the acclimation period, both WT and miR-29KO mice were randomly distributed in the above-mentioned training groups. In the first week of training, maximal endurance and resistance tests were carried out. The mice in the training groups performed a specific maximal test for the quality to be trained, while the mice in the sedentary group performed both the maximal endurance test and the maximal resistance test, 24 h apart. Maximal endurance capacity was determined by an incremental test in the treadmill and maximal resistance performance was tested in the vertical ladder, following the protocols previously described by our research group [15,16]. Both tests were repeated at the end of the training period.

2.2.3. Training

All mice trained for 4 weeks, 5 days/week (Monday to Friday). To reduce anxiety, mice were trained in groups of four, always considering mice from the same cage. Training protocols were adapted from our previous works in terms of intensity and duration of sessions [15,16]. Briefly, endurance training sessions started with identical warm-up as for the maximal endurance performance test. Then, all sessions consisted of continuous running with a mean duration of 60 min and the distance covered every day was 1000 m, as a fixed volume. The intensity in terms of maximal speed, number of stages, as well as the speed and duration of each stage, varied along the week according to this structure: 2 days at high intensity (Tuesday and Friday), 2 days at moderate intensity (Monday and Thursday), and 1 day at low intensity (Wednesday). Speed ranged from 20 to 40 cm/s, which corresponded to 40–80% of mean maximal speed at the pre-training test [17]. The duration of each stage varied inversely with speed, between 15 and 5 min [17]. The slope was fixed at 10°. In the case of resistance training, sessions started with an identical warm-up as for the maximal resistance performance test. Then, all sessions were designed to achieve the same exercise volume by means of a combination of number of steps climbed (or distance against gravity) and weight load [18]. The number of steps per training session varied between 400 and 2000, depending on the maximal weight load, which ranged between 20 and 50 g or 25–65% of the maximal weight load at the pre-training test. We selected these maximum weight ranges since below 75% of 1 repetition maximum there is no velocity loss, which is important for standardizing intensity of submaximal efforts [19]. Week planning was: 2 days with high weight

load and low number of steps (Tuesday and Friday), 2 days of intermediate weight load and number of steps (Monday and Thursday), and 1 day without weight load but a high number of steps (Wednesday). Control mice remained in a cage, in the same room, while END and RES mice were training.

2.2.4. Lactate threshold test

A maximal endurance test to determine lactate threshold was carried out in a small cohort of WT and miR-29KO mice. Blood samples were collected every 3 min by puncture from a tail vein until exhaustion. The blood lactate concentration (mM) was measured using an enzyme electrode method with Lactate PRO 2 (Arkray Inc, Kyoto, Japan) and the blood glucose concentration (mg/dL) was analyzed using Accu-Chek® Aviva glucometer (Roche, Basel, Switzerland).

2.3. Blood extraction and tissue collection

All mice were sacrificed 24 h after the last training session. Mice were deeply anesthetized with ketamine (10 mg/mL) and xylazine (1 mg/mL) in saline solution. Blood was drawn from the vena cava, using an intravascular catheter (0.9 × 25 mm; BD Insyte, 381223) pretreated with EDTA (0.5 M) as an anticoagulant. After collection, plasma was rapidly separated by centrifugation at 600×*g* for 15 min at 4 °C. Plasma samples were immediately frozen in liquid nitrogen and stored at −80 °C.

After blood sample collection, a cut was made in the abdominal aorta and all mice were perfused with 20 ml of cold PBS from the vena cava, to flush the tissues and prevent the blood interference in the ulterior tissue levels miRNA analysis.

Skeletal muscles (quadriceps and soleus) and liver of each mouse were removed. Right quadriceps and soleus were extracted, washed in PBS, cleaned of connective tissue, rapidly frozen in liquid nitrogen, and stored at −80 °C for biochemical analysis.

2.4. Sequencing of miRNAs obtained from pooled plasma samples

100 μL of plasma from 5 samples per group (CON, END and RES) were pooled, generating three pools of 500 μL each. From these pooled samples, EVs precipitation was conducted with exoRNeasy (QIAGEN, Hilden, Germany) following manufacturer`s instructions. EVs RNA was isolated with proprietary RNA isolation protocol (Exiqon Services, Denmark) optimized for serum/plasma (no carrier added). Total RNA was eluted in ultra-low volume. The library preparation was done using the QIAseq miRNA Library Kit (QIAGEN, Hilden, Germany). A total of 5 μL of the RNA was converted into miRNA Next Generation Sequencing (NGS) libraries. Adapters containing unique molecular identifiers (UMIs) were ligated to the RNA. Then, RNA was converted to cDNA using the miRCURY LNA RT kit (QIAGEN, Hilden, Germany). The cDNA was amplified using PCR (22 cycles) and during the PCR, indices were added. After PCR the samples were purified. Library preparation QC was performed using either Bioanalyzer 2100 (Agilent, Santa Clara, CA, USA) or TapeStation 4200 (Agilent). Based on the quality of the inserts and the concentration measurements, the libraries were pooled in equimolar ratios. The library pool(s) were quantified using the qPCR ExiSEQ LNA™ Quant kit (Exiqon, Denmark), and then sequenced on a NextSeq500 sequencing instrument, generating 75 np single-ended reads. Raw data was demultiplexed and FASTQ files for each sample were generated using the bcl2fastq conversion software v2.20 (Illumina inc., San Diego, CA, USA). FASTQ data were checked using the FastQC tool. Bowtie2 was used for sequence alignment against reference miRNA sequences (miRBase v20) from *Mus musculus*. Feature counting was carried out using HTSeq-count. Before expression analysis, the obtained count matrix was normalized using the Transcripts Per Kilobase Million (TPM) method. The criteria for miRNA selection were: 1) miRNAs with an expression level of 30—1000 RPM and high change compared to the CON group ($\log_2$ FC > 1.73) and 2) highly expressed miRNAs (>1000 RPM) with at least moderate relative expression change compared to CON ($\log_2$FC > 0.5) were selected [20]. The miRNAs that met these criteria were subsequently validated by RT-qPCR in each individual plasma sample (see Methods section 2.12 and Tables S1 and S2). Raw data are available on ZENODO (https://zenodo.org/doi/10.5281/zenodo.11184908).

2.5. Functional in silico analysis

Pathway analysis of the genes targeted by the EV miRNAs identified was performed to gain insight into their potential functional implication in the biological response to exercise. For each miRNA, experimentally validated targets were retrieved from miRTarBase and miRWalk databases. miRTarBase v7.0 validated gene targets were used on DIANA TOOLS miRpath v.3 using KEGG pathways union analysis [21,22]. We used target mining analysis by miRWalk v3 for gene interactions. The data downloaded from miRWalk were utilized on Cytoscape v3.10.0 to create target intersection between miRNAs.

2.6. Cell culture of mouse C2C12 cells

The mouse skeletal muscle myoblast cell line C2C12 were obtained from the American Type Culture Collection (ATCC CRL-1772). The C2C12 cell line was cultured in DMEM (Dulbecco's Modified Eagle Medium, 11965092, Gibco, Thermo Fisher Scientific, Inc., MA, USA). This media contains high levels of glucose (4.5 g/L) and L-glutamine and was supplemented with 10% fetal bovine serum (FBS, F7524, Sigma—Aldrich) and 1% antibiotic-antimycotic cocktail (10000 U/mL penicillin, 10000 μg/mL streptomycin, and 0.25 μg/mL amphotericin B, 11580486, Gibco, Thermo Fisher Scientific, Inc., MA, USA). For differentiation to myotubes, C2C12 myoblasts were seeded in a 6-well plate at a density of 2×10^6 cells/well. After two days, when cells reached 90—100% confluence, differentiation was induced by switching to DMEM supplemented with 2% horse serum (HS, H1270-500 ML, Sigma—Aldrich, St. Louis, MO, EEUU) and 1% antibiotic-antimycotic cocktail. Differentiation was monitored microscopically and cells were used for experiments after 6—7 days. The absence of mycoplasma contamination was routinely confirmed by PCR. Cells were maintained at 37 °C under 5% CO_2.

2.7. Electrical pulse stimulation (EPS)

On day 6 of differentiation, differentiated myotubes were electrically stimulated using the C-Pace EP cell culture stimulator with carbon electrodes (EPS; C-Pace EP; Ionoptix, MA, USA) [23]. To simulate basal exercise conditions, 24 h before electrostimulation, the culture media was changed to DMEM with low glucose concentration (1 g/L) and EVs-free HS to avoid contamination of EVs. Both electrostimulated and control cells remained in this media during the protocol. The EPS protocol consisted of applying pulses continuously (2 ms) to the myotubes at 1 Hz and 40V for 3 h in the incubator (at 37 °C and 5% CO_2). The contractions of the myotubes were observed under a microscope. Both the electrostimulation and control plates remained with the electrodes. However, in the case of the controls, there was no stimulation. Once the simulation period was completed, the medium samples were collected for EVs isolation, the plates were washed with PBS and cell lysis performed 0, 3 and 20 h after EPS.

2.8. MiR-29a-3p inhibitor transfection

C2C12 cells were transfected with two different concentrations (15 nM or 100 nM) of mmu-miR-29a-3p MirVana inhibitors or a negative control inhibitor (Life Technologies, Carlsbad, CA, USA), 2 days after induction of differentiation. Transfection at the same concentration was

repeated at 48 h. Each transfection was performed for 24 h in Opti-MEM™ I Reduced-Serum Medium (31985062, Gibco, Thermo Fisher Scientific, Inc., MA, USA) with Lipofectamine™ RNAiMAX Transfection Reagent (13778150, Invitrogen, Thermo Fisher Scientific, Inc., MA, USA). This is an improved Minimal Essential Medium (MEM) that allows for a reduction of FBS supplementation by at least 50% with no change in growth rate or morphology. The transfection efficiency of the different concentrations of miR-29a-3p inhibitors was estimated by qPCR, reflecting the inhibition activity of the different concentrations of miR-29a-3p inhibitors. Considering the transfection efficiency, the 100 nM concentration was selected for a second protocol in which, after transfection on days 2 and 4 of differentiation, cells were electrostimulated on day 6, following the same protocol described before.

2.9. Cell viability

The lactate dehydrogenase (LDH) release assay was used as a colorimetric method to estimate cell cytotoxicity. The presence of LDH in the extracellular media reveals a defect in cell membrane permeability due to cell death. Briefly, cells were exposed to EPS protocol for 3 h under normal conditions and under conditions of miR-29a-3p inhibition. 100 μL of the supernatant from each condition was transferred to a 96-well plate and 100 μL of LDH assay reagent consisting of a dye and a catalyzer were added to each well. After an incubation period of 30 min under shaking at room temperature, the absorbance was measured at 490 nm using microplate Versa Max Plate reader (MolecuarDevices, San Jose, CA, USA). The absorbance at 690 nm was also measured as a reference for the background of each well.

As a positive control, 20 μL of a 0.1% Triton solution was added to the cells for 4 h in the incubator at 37 °C. Cells were then lysed and centrifuged at 500×*g* for 5 min to remove cell debris. The supernatant was used as positive control. Cell death was expressed as the percentage of cytotoxicity with respect to the positive control for each condition.

2.10. Collection of cell culture samples

From the culture media of each of the plates (approximately 12 mL), EVs were isolated using total EV isolation reagent (exosome-enriched) (4478359, Thermo Fisher Scientific, Inc., MA, USA). The reagent was added to the total volume of culture media at a ratio of 1:2 and the solution was incubated overnight at 4 °C. Precipitated exosomes were recovered by standard centrifugation at 10,000×*g* for 60 min. An aliquot of the supernatant was taken as a negative control for the presence of EVs and the remainder was removed. The pellet was resuspended in 200 μL of modified PBS (HyClone Dulbecco's phosphate buffered saline: liquid, Cytiva SH30028.02, Thermo Fisher Scientific, Inc., MA, USA), an aliquot was used to measure protein concentration by BSA technique, and the remainder was frozen at −80 °C until use.

After removal of the culture media, cells were washed with PBS (1X) and used to extract RNA (2×10^6 cells). 700 μL of Qiazol lysis reagent (QIAGEN, Hilden, Germany) was added to the cell culture plate. Cells were detached using a scraper and transferred to 1.5 mL tubes. The content was shaken vigorously with the vortex for 1 min for further analysis.

2.11. Total RNA extraction

2.11.1. miRNA extraction from plasma EVs

The remaining plasma volume from CON, END, and RES mice, not used for NGS, was treated with thrombin to create serum like samples (SBI, Palo Alto, CA, USA). SeraMiR Exosome RNA purification kit (SBI, Palo Alto, CA, USA) was used to facilitate EVs precipitation and extraction. miRCURY RNA isolation kit (QIAGEN, Hilden, Germany) was used to extract miRNAs from 200 μL of plasma samples following the manufacturer's instructions. The RNA Spike-in kit (QIAGEN Hilden, Germany), which contains synthetic RNA spike-in templates UniSp2, UniSp4, and UniSp5, was used in all extractions to control the efficiency of RNA isolation. RNA was eluted in 30 μL RNase-free H_2O and its concentration measured by NanoDrop (Thermo Fisher Scientific, Inc., MA, USA), before samples were stored in a −80 °C freezer.

2.11.2. RNA extraction from cell culture EVs

RNA extraction from EVs obtained from the culture media was performed using the Total Exosome RNA & Protein Isolation Kit (4478545, Invitrogen, Thermo Fisher Scientific, Inc., MA, USA). RNA concentration was measured by Nanodrop and stored at −80 °C.

2.11.3. RNA extraction from mouse tissues and C2C12 cells

RNA extraction was performed from 50 mg of quadriceps, 25 mg of liver, 5 mg of soleus and 2×10^6 C2C12 cells in dry ice conditions. Tissues were disrupted using a mortar and pestle with 700 μL of Qiazol lysis reagent (QIAGEN, Hilden, Germany). MiRNeasy mini kit (QIAGEN, Hilden, Germany) for quadriceps, liver, and cell pellet, and miRNeasy micro kit (QIAGEN, Hilden, Germany) for soleus were used to extract total RNA following the manufacturer's instructions. RNA was eluted in 30 μL RNase-free H_2O. All samples were measured by NanoDrop (Thermo Fisher Scientific, Inc., MA, USA) and stored at −80 °C to further analysis.

2.12. miRNA expression analysis by RT-qPCR

For plasma EVs, 2 μL RNA samples were reverse transcribed in 10 μL reaction. For tissue, EVs and C2C12 cells analysis equal quantities of RNA (5 ng/μL) were used. cDNA was synthesized using the miRCURY LNA RT kit (QIAGEN, Hilden, Germany) [24]. Additional spike-in (UniSp6) (QIAGEN, Hilden, Germany) was added to the cDNA synthesis reaction to check for RT and PCR inhibitors. RT reaction was performed with the following conditions: incubation for 60 min at 42 °C, heat-inactivation for 5 min at 95 °C, immediately cool to 4 °C. For qPCR, cDNA was diluted 1:40 and 4 μL used in 10 μL with miRCURY LNA SYBR Green PCR master mix (QIAGEN, Hilden, Germany) on a 7900HT fast real-time PCR system (Applied Biosystems, Waltham, MA, USA) with the following cycling conditions: 10 min at 95 °C, 40 cycles of 10 s at 95 °C and 1 min at 60 °C, followed by melting curve analysis. Primers for miRNAs were obtained from Qiagen (Table S3). EV samples were analysed in technical triplicates and Ct values were averaged for each miRNA. Relative levels of miRNAs and were quantitatively analysed using the $2^{-\Delta\Delta Ct}$ method [25]. Normalization of circulating EV miRNAs was performed using the mean expression of all miRNAs analysed, given that more than 50 miRNAs were evaluated [26]. At tissue, cellular, and EV secreted by cells levels, based on the equal amounts of RNA added, an external normalizer, UniSp6, was used to reduce possible technical errors.

2.13. mRNA expression analysis by RT-qPCR

cDNA was synthesized using the StaRT Reverse Transcription kit (AnyGenes, Paris, France) for mRNA. For tissue analysis, equal quantities of RNA (500 ng) were used. For mRNA, cDNA was diluted 6-fold and 1 μL was used in 10 μL qPCR reactions with the Perfect Master Mix SYBR Green kit (AnyGenes, Paris, France) in the 7900HT real-time PCR system (Applied Biosystems, Waltham, MA, USA), with the following cycling conditions: 10 min at 95 °C, 40 cycles of 10 s at 95 °C and 30 s at 60 °C and 1 min at 60 °C, and 30 s at 65 °C. Relative levels of genes were quantitatively analyzed using the $2^{-\Delta\Delta Ct}$ method [25]. Primers for the genes analyzed were specifically designed by AnyGenes; the information is listed in Table S4. *β-actin* and *Gapdh* were used as housekeeping genes for mRNA expression (Table S4).

2.14. Western blotting

20 mg of quadriceps or 5 mg of soleus were homogenized with the aid of a 2 mL Potter-Elvehjem homogenizer (432-0200, VWR, Radnor, Pennsylvania, USA) in 400 μL or 100 μL of homogenization buffer, respectively. This buffer consisted of 20 mM HEPES, pH 7.4, 100 mM NaCl, 50 mM NaF, 5 mM EDTA, 1 % Triton X-100, 1 mM sodium orthovanadate, 1 mM pyrophosphate and 1X CompleteTM Protease Inhibitor Cocktail (CO-RO Roche Life Science, Basel, Switzerland). Samples were then centrifuged at 12,000 × *g* at 4 °C for 10 min and the supernatant was collected and stored at −80 °C until use. For EVs samples, 200 μL of sample containing EVs dissolved in PBS 1X were homogenized by sonication with continuous 35% pulses of 10 s on and 5 s off for 1 min.

Protein quantification was determined by Nanodrop. Total protein (30—50 μg of tissue and 10 μg of cell pellet and EVs) was resuspended in loading buffer (BR5X) (300 mM Tris/HCl, pH 6.8, 10% SDS, 50% glycerol, 20% 2-mercaptoethanol, 40 mM EDTA and 0.05% bromophenol). Prior to gel loading, samples were boiled in a thermoblock for 5 min at 95 °C s) and loaded onto 4—12% precast Bis-Tris gels (MP41G12, MerckMillipore, Darmstadt, Germany). Prestained Protein Ladder marker with a range of 5—245 kDa (AB116029, Abcam, Cambridge, UK) was used. Proteins were transferred to PVDF membranes (pore size of 0.2 μm, 15239814, Amersham Hybond™, Amersham, UK). Transfer was carried out wet with the transfer buffer at a constant amperage of 250 mA at 4 °C. Then, membranes were incubated in blocking solution [5% bovine serum albumin (BSA), in TBS-T (200 mM Tris/HCl, pH 7.6, 1.5M NaCl and Tween 20)] at room temperature and shaking. After blocking, membranes were incubated with the corresponding primary antibody (Table S5) in TBS-T 1X overnight at 4 °C and shaking. Next day, the membranes were washed with TBS-T 1X and incubated with the appropriate horseradish peroxidase-conjugated secondary antibodies (Table S5) for 1 h at room temperature. Detection was performed using Amersham ECL Prime Western Blotting Detection Reagent (Cytiva, MA, USA). Chemiluminescence was captured using VisionWorksLs software (UVP, CA, USA). For normalization, immunoblots were quantified with ImageJ version 1.6 (Fiji), with either beta-Actin or Gapdh as loading controls.

2.15. Statistical analysis

Unless otherwise specified, data are presented as mean ± SEM and represented as column scatter plots. Normality of the variables was tested by means of the Shapiro—Wilk test. Thus, for the variables that met these assumptions, Student's t-test for unpaired or paired samples, and analysis of variance (ANOVA), followed by a Tukey's post hoc test, were applied, depending on the number of groups to be compared. Pearson's or Spearman's correlation coefficient was calculated to explore associations between variables, and data were corrected for multiple testing with FDR (Benjamini and Hochberg). *p*-value ≤0.05 was considered significant, and it is shown in each graph. Analyses were performed using either SPSS software version 27 for Windows (IBM, Armonk, NY, USA), GraphPad Prism version 8.0.1 for Windows (GraphPad, San Diego, CA, USA) or R 4.0.2 (www.r-project.org).

3. RESULTS

3.1. Next-generation sequencing revealed a specific EV-miRNA profile in response to resistance training, functionally grouped in two clusters

With the aim of screening the miRNA profile contained in plasma EVs in response to training, a 4-week exercise intervention, consisting of endurance (END) or resistance (RES) training, was designed and implemented in C57BL/6N 12-week-old male mice (Figure 1A), following our previously described protocols [15,16]. Another group of mice did not undergo any training during this period (CON). Endurance and resistance maximal capacities were determined by incremental tests (see 2.2.2 section), before and after the intervention. END and RES mice improved their capacity trained, while CON mice maintained their resistance capacity but worsened their aerobic endurance performance (Figure 1B—D).

Since miRNAs present in EVs have been shown to participate in systemic crosstalk during exercise [2,27], total RNA, including small RNAs, was extracted from previously isolated EVs of pooled plasma samples ($n = 5$/group) (Fig. S2). Short RNA NGS was then performed. We identified 223 miRNAs with a minimum expression of 1 TPM in at least one sample [28]. From them, 54 miRNAs met the selection criteria, as described in section 2.5, and were validated by RT-qPCR in each plasma sample (Table S2). In these samples, we found that 11 training-associated miRNAs were upregulated in RES mice relative to CON (Figure 2A). Ten of them were significantly increased: mmu-miR-10b-5p, mmu-miR-30a-5p, mmu-miR-126a-3p, mmu-miR-126a-5p, mmu-let-7a-5p, mmu-miR-29a-3p, mmu-miR-143-3p, mmu-let-7i-5p, mmu-miR-142a-5p and mmu-let-7c-5p, whereas mmu-let-7f-5p showed a notable, although not significant, increase ($p = 0.056$) (Figure 2B).

We then performed an in-silico analysis, using DIANA-miRPath v.3.0, to identify the main integrated metabolic pathways in which these 11 miRNAs are involved (Figure 2C). This analysis revealed several metabolic processes associated with the response to exercise and allowed us to identify two different clusters. Cluster 1 consisted of let-7a-5p, let-7c-5p, let-7i-5p and let-7f-5p, and miR-29a-3p, with 286 common targets (Figure 2D), involved in different signaling pathways such as AMPK, PI3K-Akt and mTOR. Cluster 2 included miR-10b-5p and miR-30a-5p, with 30 common targets (Figure 2E), having an important role in central fat metabolism, fatty acid and steroid biosynthesis.

Taking together, these results show that resistance training increases the expression of a EV miRNA signature. The existence of two functional clusters suggests a coordinated response of these EV miRNAs for the physiological modulation of energy metabolism in the adaptation to resistance training.

3.2. Modulation of the EV miRNA signature in skeletal muscle in response to training suggests its role in EV miRNA trafficking during exercise

To better understand whether skeletal muscle is involved in tissue-to-tissue communication in response to training through miRNA release as EV cargo, we next evaluated the expression levels of the miRNA signature identified in plasma in two different types of skeletal muscles: soleus and quadriceps.

In soleus, most of the training-associated miRNAs showed reduced expression levels in both END and RES compared to CON (Figure 3A—C). However, three of them presented a specific response to endurance training: let-7c-5p and miR-142a-5p, displaying lower expression, and let-7f-5p, showing higher expression (Figure 3A,C). No differences were observed in quadriceps (Figure 3D—F).

No significant correlations were observed between miRNA expression levels in EVs and in muscle tissues in END, RES or CON (Fig. S3A—D). In addition, no significant correlations were found among the relative expression levels of training-associated miRNAs in soleus of any group of mice (Figure 3G). Interestingly, miR-29a-3p expression in quadriceps of RES mice showed a positive and significant correlation with let-7i-5p ($\rho = 0.85$, FDR = 0.019), miR-126a-3p ($\rho = 0.95$,

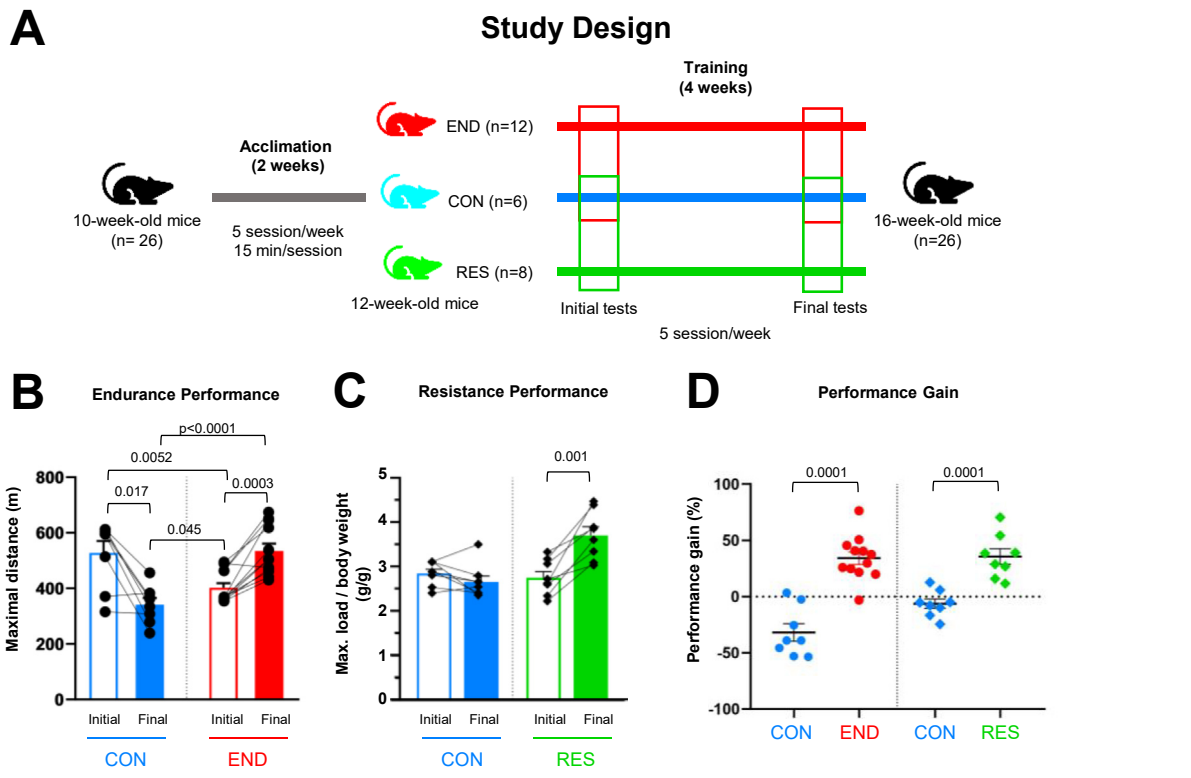

Figure 1: Endurance and resistance performance in WT mice. A. Schematic representation of the training intervention study design (sedentary, CON; endurance, END; and resistance, RES). **B—C.** Endurance and resistance performance before (Initial) and after (Final) training intervention in CON *vs.* END (B) and CON *vs.* RES (C). **D.** Performance gain of, measured as percent variation (%). Statistical significance was determined by a paired (B and C) or unpaired (D) two-tailed *t*-test and *p*-values are indicated in the figures. Data are presented as mean or percentage mean ± SEM. Each dot represents one mouse. CON ($n = 6$), END ($n = 12$), and RES ($n = 8$).

FDR = 0.004), miR-143-3p ($\rho = 0.90$, FDR = 0.009), and miR-30a-5p ($\rho = 0.95$, FDR = 0.004) levels (Figure 3H). Furthermore, regarding the relationship between miRNA tissue levels and performance parameters, we found a negative correlation between resistance performance gain and the relative expression levels in quadriceps of miR-29a-3p ($\rho = -0.81$, FDR = 0.034), miR-10b-5p ($r = -0.80$, FDR = 0.028), let-7c-5p ($r = -0.80$, FDR = 0.028), let-7f-5p ($\rho = -0.90$, FDR = 0.009), let-7i-5p ($\rho = -0.88$, FDR = 0.014), miR-126a-3p ($r = -0.78$, FDR = 0.034), miR-143-3p ($r = -0.73$, FDR = 0.050), and miR-30a-5p ($r = -0.76$, FDR = 0.039) (Figure 3I). In summary, the training-associated EV miRNAs were also detected in skeletal muscle of trained and untrained mice, suggesting this tissue as a potential source of these miRNAs in plasma EVs. Additionally, their response to training was different according to the training model and the muscle type, highlighting the role of miR-29a-3p in this adaptive process.

3.3. miR-29a-3p is secreted in EVs by mouse myotubes in response to electrostimulation and has a potential modulatory effect on the secretion and intracellular expression of other training-associated miRNAs

To explore the possibility that miRNAs present in circulating EVs were secreted by skeletal muscle cells, we used the mouse myoblast cell line C2C12, which expresses contractile proteins associated with type II muscle fibers, and has been described as one of the most suitable models for exercise response studies [23]. After differentiation of myoblasts to myotubes, they were maintained for 3 h with or without electrical pulse stimulation (EPS) to induce contractions, as a simulation of exercise [23]. Then, both myotubes and culture media were collected at three different time points, 0, 3, and 20 h after EPS, to isolate EVs (Fig. S4A) for miRNA determination (Figure 4A).

Most of the training-associated miRNAs identified in plasma EVs and skeletal muscle were also detected in the *in vitro* model (Figure 4B—D and Fig. S4B—E). On the contrary, miR-126a-3p, miR-126a-5p, miR-142a-5p, and miR-10b-5p were not detected, most likely because the main source of these four miRNAs is not of muscle cell origin. Indeed, miR-126a-3p and miR-126a-5p are mainly expressed in endothelial cells [29], the main mononuclear cell type in muscle, but not in myotubes [30], and, in the case of miR-142a-5p and miR-10b-5p, their absence in the C2C12 cells had already been observed by other authors [31].

Of the miRNAs analyzed that showed expression changes in EPS C2C12 cells compared to unstimulated cells, different dynamics were observed. Thus, miR-30a-5p significantly increased its expression in culture media-EVs immediately at the end of the EPS period (Figure 4B). In contrast, the response of let-7f-5p was more delayed, as it significantly decreased in EVs and tended to increase at the intracellular level 20 h after the end of EPS (Figure 4C). Finally, miR-29a-3p dynamics showed a tendency to be more spaced in time, as its expression was lower in EPS myotubes at Time 0 and higher in EVs 20 h after EPS (Figure 4D). This miR-29a-3p response is similar to our observations *in vivo*, as its expression in plasma EVs increased 24 h after the last training session (Figure 2A—B) and decreased in soleus in trained mice (Figure 3A).

Next, we performed a downregulation study in C2C12 cells using a miR-29a-3p specific inhibitor (miR29dKD cells; Fig. S5A). We first confirmed the inhibition of miR-29a-3p and the decrease in the expression of the other family members, miR-29b-3p and miR-29c-3p

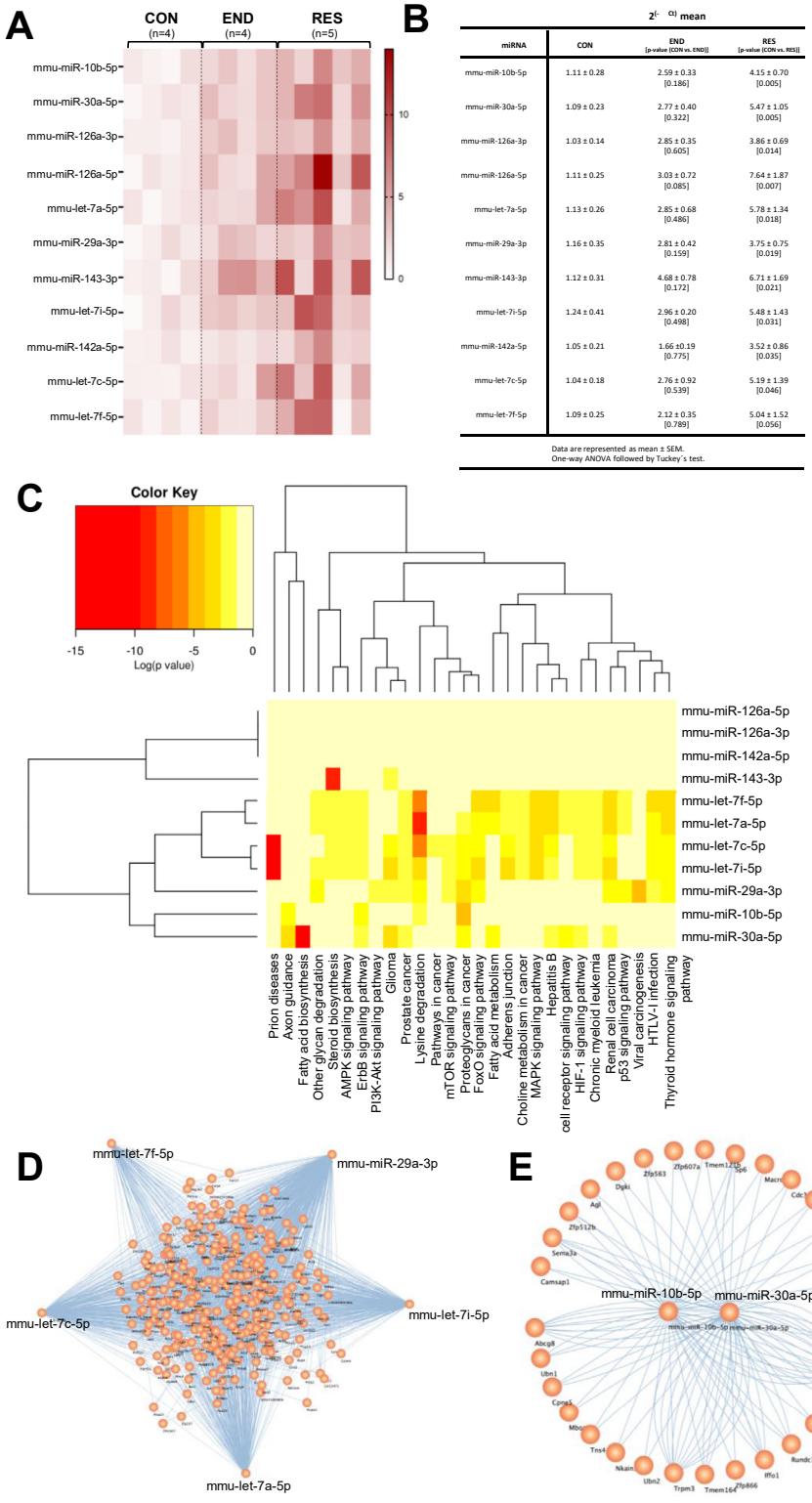

Figure 2: Training-associated miRNA profile in extracellular vesicles (EVs), main KEEG pathways and functional miRNA clusters. A. Heatmap of the differentially expressed miRNAs identified by NGS and validated by RT-qPCR. Each row represents one miRNA, and each column represents an individual mouse within each group CON ($n = 4$), END ($n = 4$) and RES ($n = 5$). The relative expression levels ($2^{(-\Delta\Delta Ct)}$) are shown in colors, from white (low) to dark red (high). **B.** Table with the relative mean expression of the 11 training-associated miRNAs differentially expressed and *p*-values. Statistical differences between CON and trained groups were measured by one-way ANOVA followed by Tuckey's post hoc test. Data are presented as mean ± SEM. **C**. Heatmap of the pathway's union analysis based on the validated targets of the 11 training-associated miRNAs, grouped by functional clusters. The heatmap represents as logarithm (*p*-value) the probability of interaction of each miRNA with a specific pathway in *Mus musculus*. Significance levels are shown in different colors, ranging from yellow (low) to red (high). **D-E**. Cytoscape representation of miRWalk gene regulatory networks of the miRNAs belonging to clusters 1 (D) and 2 (E) in *Mus musculus*. (For interpretation of the references to colour in this figure legend, the reader is referred to the Web version of this article.)

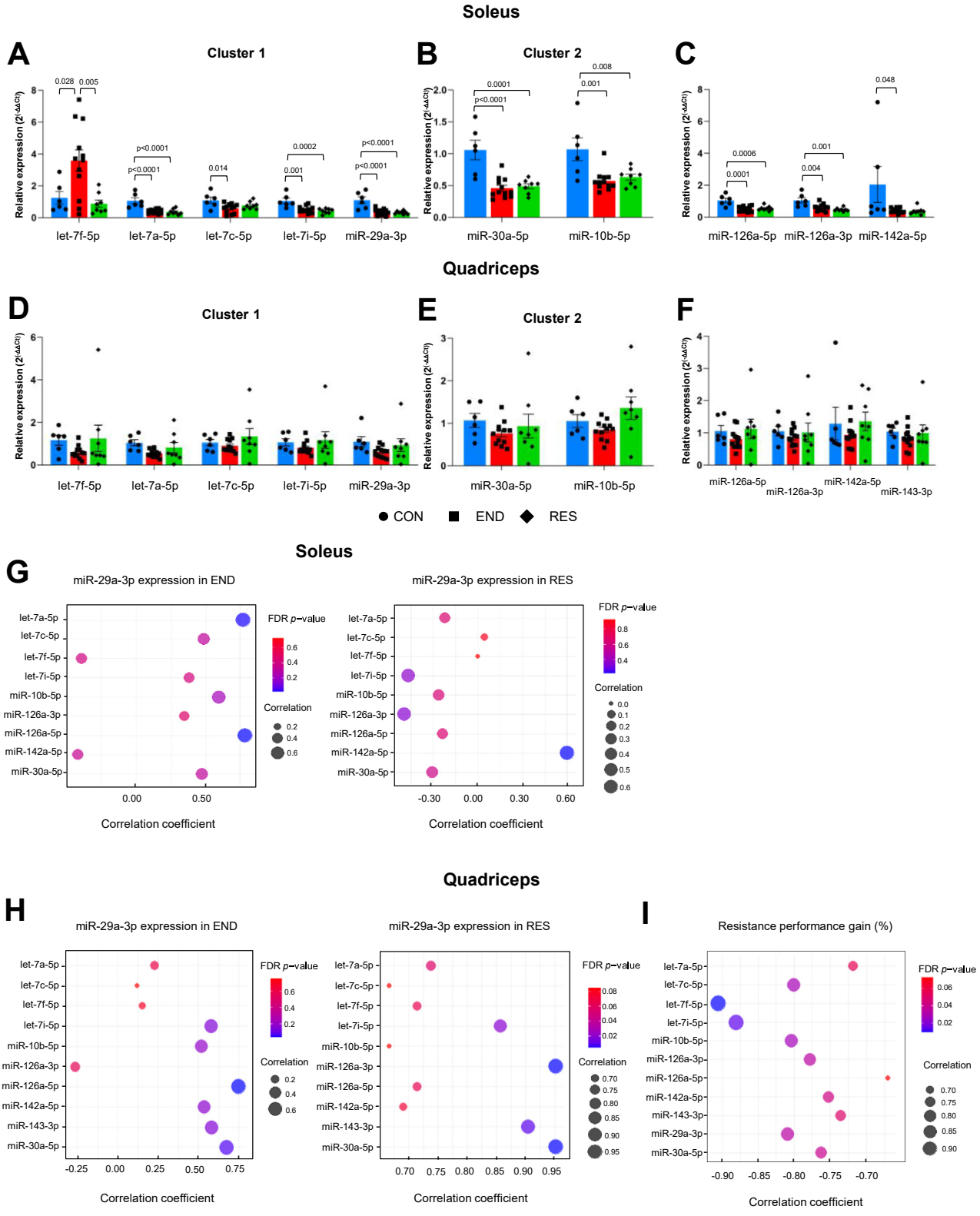

Figure 3: Modulation of the EV miRNA signature in skeletal muscle in response to endurance and resistance training. A-F. Relative expression levels of miRNAs from clusters 1, 2, and unclustered miRNAs in the soleus and in the quadriceps. Data are presented as mean ± SEM. Each dot represents one mouse. CON, $n = 6$; END, $n = 12$ and RES, $n = 8$. Statistical significance was measured by one-way ANOVA followed by Tuckey's post hoc test and p-values are indicated in figures. (G) Correlation of miRNA expression in quadriceps of RES and performance gain (%) ($n = 8$). (H) Correlation between miRNA expression in soleus of END ($n = 12$) and RES ($n = 8$). (I) Correlation between miRNA expression in quadriceps of END ($n = 12$) and RES ($n = 8$). The size of the bubbles represents the magnitude of the correlation, while the colour of each bubble indicates the FDR adjusted p-values. (For interpretation of the references to colour in this figure legend, the reader is referred to the Web version of this article.)

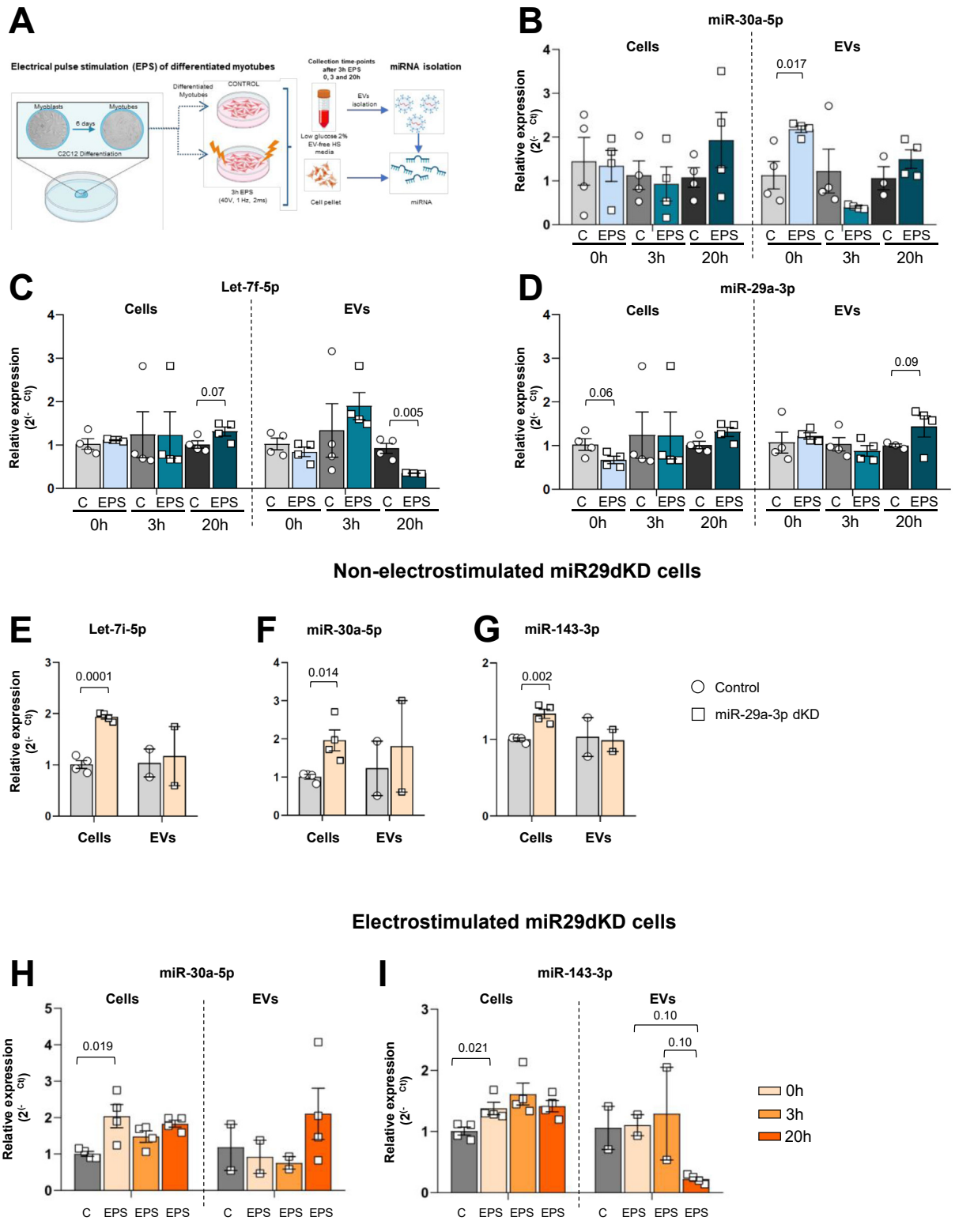

Figure 4: *In vitro* study of the impact of EPS in miRNA secretion and the modulatory effect of miR-29a-3p inhibition in training-associated miRNAs in mouse myotubes. A. Schematic representation of electrostimulation protocol on C2C12 cells and isolation of miRNAs from EVs and cells. Created with BioRender. **B-D.** Relative expression levels of miR-30a-5p, let-7f-5p, and miR-29a-3p in cells and EVs at 0, 3, and 20 h after electrostimulation in non-electrostimulated (C, $n = 4$) and electrostimulated (EPS, $n = 4$) cells. **E-G.** Relative expression of cluster 1 miRNAs (**E**), let-7i-5p (**F**), and miR-143-3p (**G**) in C2C12 myotubes where miR-29a-3p expression was inhibited by 70% (miR29dKD, $n = 4$) and in control myotubes (Control, $n = 4$). **H—I.** Relative expression of miR-30a-5p and miR-143-3p in non-electrostimulated (C, $n = 4$) and electrostimulated (EPS, $n = 4$) miR-29a-3p dKD cells at 0, 3, and 20 h after electrostimulation. Statistical significance was determined using unpaired, two-tailed Student's *t*-test and *p*-values are indicated in the figures. Data are represented as mean ± SEM. Each dot represents the mean technical duplicate of each cell replicate.

(Fig. S5B), due to sequence similarities [32]. Then, we tested whether miR-29a-3p downregulation modulated the expression of other training-associated miRNAs, both intracellularly and in EVs. At intracellular level, miR-29a-3p repression increased the expression of let-7i-5p, from cluster 1 (Figure 4E), miR-30a-5p, from cluster 2 (Figure 4F), and the unclustered miR-143-3p (Figure 4G). However, when assessing the presence of these miRNAs in EVs, downregulation of miR-29a-3p did not appear to affect either let-7i-5p, miR-30a-5p, or miR-143-3p (Figure 4E—G). Finally, EPS was applied to miR29dKD cells. In the absence of miR-29a-3p, EPS did not reverse the intracellular downregulation of the miR-29 family (Fig. S5C—D). However, miR-30a-5p and miR-143-3p further increased their expression at the intracellular level (Figure 4H—I). Considering EV secretion, the absence of miR-29a-3p appeared to block miR-30a-5p export in EVs after EPS (Figure 4H). Similarly, miR-143-3p showed a tendency to a compromised secretion in EVs at 20 h post EPS in the absence of miR-29a-3p (Figure 4I).

These results show that miR-29a-3p and miR-30a-5p are secreted in EVs by cultured skeletal muscle cells in response to electrostimulation, although with different dynamics. The fact that in the absence of miR-29a-3p the intracellular expression of miR-30a-5p and miR-143-3p increased further after electrostimulation but shows a tendency to decrease in EVs, mainly regarding miR-143-3p, suggests that this EV secretion of members of different functional clusters could be modulated in an interdependent manner in response to the contractile stimulus.

3.4. *miR-29a/b1*-deficient mice show a decreased physical capacity, particularly resistance, and a dysregulated expression of training-associated miRNAs in EVs and quadriceps

The *in vitro* results showed that miR-29a-3p is secreted by mouse myotubes in EVs in response to electrostimulation. Thus, to further study miR-29a-3p potential functional role, we used a systemic *miR-29a/b1* cluster knock-out mouse (miR-29KO). This model is characterized by a life expectancy of ~30 weeks, with a degenerative phenotype starting at 16 weeks of age [13].

We evaluated both endurance and resistance physical capacity in a group of 16-week-old miR-29KO mice and their WT counterparts. Although both capacities were affected, this effect was greater in resistance (53% mean loss) than in endurance (25% mean loss) (Figure 5B—C). This suggests that *miR-29a/b1* may play a more critical role in resistance than in endurance capacity.

Our results confirmed the lack of expression of miR-29a-3p in EVs, quadriceps, and soleus of miR-29KO mice. Interestingly, miR-29b-3p also followed the same pattern. However, miR-29c-3p only showed a decrease in soleus, with no changes in EVs or quadriceps (Figure 5A). This indicates that miR-29b1 is likely the main form of miR-29b-3p that is expressed in these structures.

We also analyzed the expression of other training-associated miRNAs in the absence of *miR-29a/b1* cluster at the systemic level. As observed in C2C12 miR29dKD myotubes, these miRNAs showed a dramatic reduction in their expression levels in EVs of miR-29KO mice relative to WT, except miR-10b-5p (Figure 5D). Regarding skeletal muscle, the observed response appeared to be dependent on the type of muscle. Thus, an increased expression of let-7c-5p, let-7i-5p, let-7a-5p, miR-126a-5p, miR-126a-3p, and miR-143-3p were detected in quadriceps of miR-29KO mice (Figure 5E). Meanwhile, in soleus, miR-30a-5p presented lower expression levels miR-29KO mice (Figure 5F).

To compare these results with those obtained in the *in vitro* model, we plotted the relative expression levels of those miRNAs whose expression changed significantly in the skeletal muscles of miR-29KO mice and were also detected in miR29dKD cells (Figure 5G). Overall, the *in vitro* model showed more similar behavior to the quadriceps, as observed for let-7c-5p, let-7i-5p, miR-30a-5p and miR-143-3p, while let-7a-5p was more similar to the soleus.

Therefore, the lack of expression of the *miR-29a/b1* cluster in an *in vivo* model strongly influences physical performance, particularly resistance, and affects the secretion in EVs and the intramuscular expression of other training-associated miRNAs, suggesting a coordinated response, as observed in the *in vitro* model.

3.5. The absence of *miR-29a/b1* increases energy substrate bioavailability but not oxidative potential in muscle tissue, leading to loss of physical performance

A shift in energy fuel utilization from fatty acid-based to glucose consumption-based metabolism was previously described in cardiac tissue of this murine miR-29KO model, with an increased expression of the ubiquitous glucose transporter *Glut1* [13]. This exacerbation of glucose metabolism, related to the positive regulation of several key enzymes in this pathway, was also observed in the liver tissue of these miR-29KO mice [13]. Therefore, we analyzed *Glut1* expression and higher levels were observed in soleus (Figure 6A) and liver (Fig. S6A), but not in quadriceps (Figure 6A), of miR-29KO mice compared to their WT counterparts. On the contrary, the inducible transporter *Glut4* showed higher expression levels in the quadriceps of miR-29KO, but not in soleus (Figure 6B), although this was not accompanied by changes at protein level (Figure 6C). We also determined the expression of phosphofructo-1-kinase (*Pfkm*), the main regulatory enzyme of the glycolytic pathway. *Pfkm* expression was higher in both muscle tissues of miR-29KO mice, although only significant in quadriceps (Figure 6D). Thus, it seems that glucose transport and its glycolytic utilization in skeletal muscle is regulated differently in the absence of *miR-29a/b1*, consistent with that previously described for cardiac muscle and liver [13].

In light of this result, we conducted a lactate threshold test in another cohort of 16-week-old miR-29KO and their corresponding WT mice, in which blood lactate and glucose levels were determined every 3 min during the test. No differences were detected in basal lactate concentration between genotypes (Fig. S6B). However, while lactate levels remained stable during the test in miR-29KO mice, a significant 65% increase (or 1.7 ± 0.8 mM) was observed in WT mice. In line with what was previously described [33], the increase in lactate observed in WT was not linear, and lactate accumulation began after 200 m, at the beginning of the 35 cm/s step, corresponding to a lactate concentration of 3.73 ± 1.2 mmol/L, and reaching a maximum concentration at the end of the test of 4.8 ± 0.2 mmol/L. No changes in glucose levels were observed during the test in miR-29KO mice (Fig. S6C), while there was a tendency to increase in WT mice between the beginning and the end of the test (12% increase or 22 ± 16 mg/dL, $p = 0.055$). This suggests that *miR-29a/b1* cluster deficiency could be affecting the transition from aerobic to anaerobic metabolism, due to a differential profile of substrate use, in line with the previous observation.

The low blood lactate levels measured in miR-29KO mice during exercise may indicate that it is being used as a gluconeogenic substrate at the hepatic level. Indeed, we have observed higher liver expression of fructose-1,6-bisphosphatase 1 (*Fbp1*), an important enzyme of gluconeogenesis, in miR-29KO mice compared to WT (Fig. S6A).

Besides the alterations in glucose availability and use, we explored the expression of genes involved in fatty acid transport and metabolism. Thus, we observed that *Scl27a4* and *Scl27a1* fatty acid transporters were overexpressed in soleus and liver of miR-29KO mice (Figure 6E and Fig. S6D), with a tendency to higher protein levels of Acsvl4 in

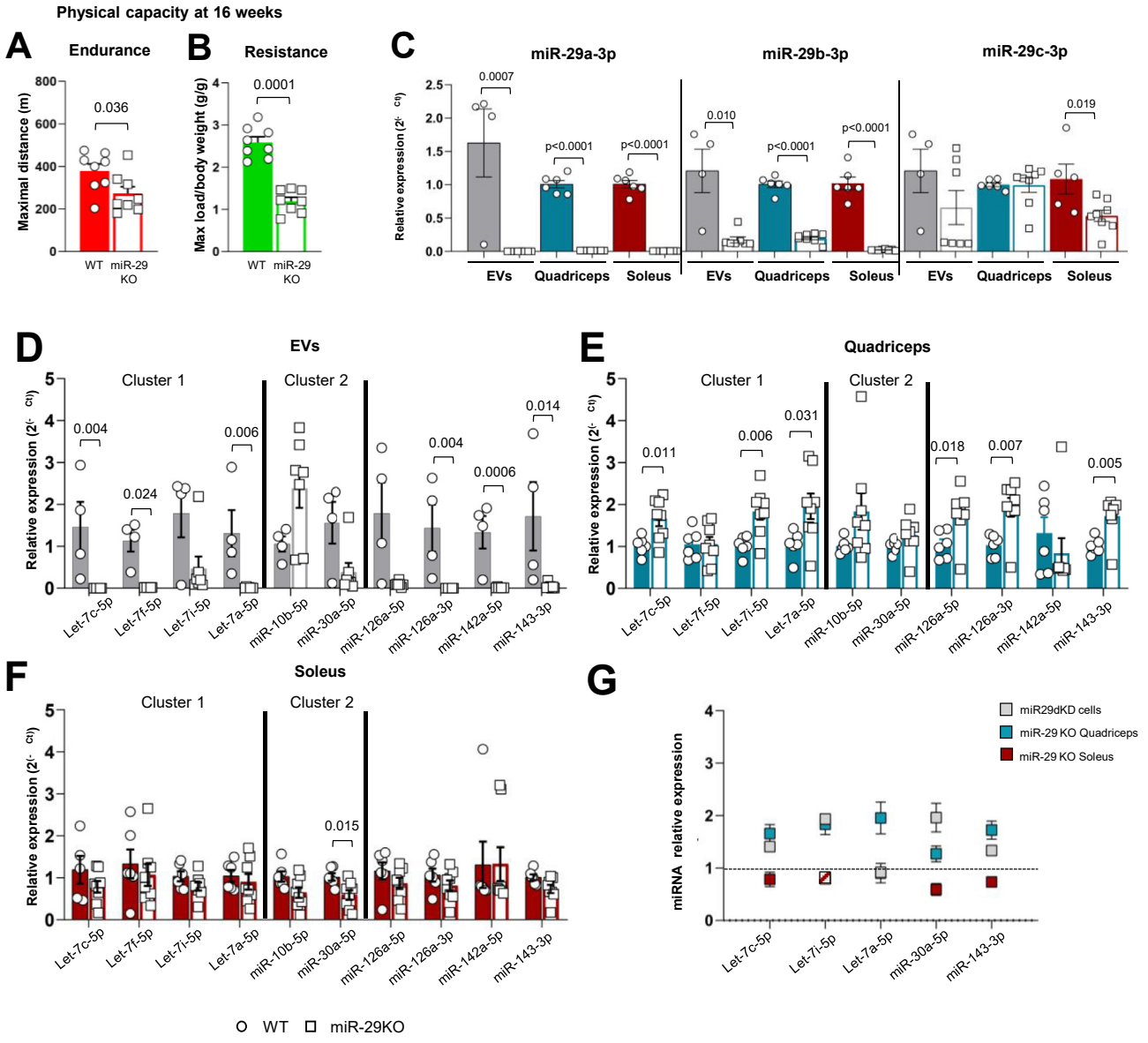

Figure 5: ***MiR-29a/b1*** **knockout mice show low resistance capacity and an altered training-associated miRNA profile in skeletal muscle. A.** Relative expression levels of miR-29 family members in EVs, quadriceps, and soleus of 16-week WT and miR-29KO mice. WT (EVs, $n = 4$; skeletal muscle tissue, $n = 6$), miR-29KO KO (Evs and skeletal muscle tissue, $n = 8$). **B—C.** Endurance and resistance performance of 16-week WT and miR-29KO mice (WT, $n = 8$; miR-29KO, $n = 8$). Data are presented as percentage mean ± SEM. **D-F.** Relative expression levels of the 11 training-associated miRNAs organized by clusters in EVs, quadriceps, and soleus of 16-week WT and miR-29KO mice. WT (EVs, $n = 4$; skeletal muscle tissue, $n = 6$), miR-29KO KO (Evs and skeletal muscle tissue, $n = 8$). **G.** Relative miRNA expression in quadriceps and soleus of miR-29KO mice *vs.* miR29dDK myotubes differentiated *in vitro* ($n = 8$ independent samples of tissue and $n = 4$ independent samples of cell culture). Statistical significance was determined using unpaired, two-tailed Student's *t*-test and *p*-values are indicated in the figures. If not indicated otherwise, data are presented as mean ± SEM. Each dot represents one mouse.

soleus (Figure 6F). However, no differences in mRNA or protein levels were observed in quadriceps (Figure 6E—F). Regarding β-oxidation enzymes, *Acadvl*, a very long-chain acyl-CoA dehydrogenase, and *Acadm*, a medium-chain acyl-CoA dehydrogenase, were studied. *Acadvl* presented higher relative expression levels in skeletal muscle and liver in miR-29KO mice (Figure 6G and Fig. S6E), although we have not found changes at the protein level in muscle tissue (Figure 6H). *Acadm* also showed higher expression levels in the liver of miR-29KO mice (Fig. S6E), but not in the quadriceps or soleus (Figure 6G). Interestingly, no changes in the relative expression of fatty acid synthase, *Fasn*, was detected (Figure 6I and Fig. S6F). Our findings align with those of Caravia et al. [13], who reported similar results in the liver of the same miR-29KO model. However, these authors found a decreased expression of *Acadvl* gene in the cardiac tissue in this model, highlighting a tissue-dependent role for *miR-29a/b1* in regulating fatty acid metabolism. Taken together, these findings suggest that in 16-week-old sedentary miR-29KO mice there is an exacerbation in the availability of energy substrates in skeletal muscle and liver compared to their WT counterparts in the resting state. The observed response in the liver of these mice may be partially attributed to dysregulation of the other two miR-29 family members (Fig. S6H) and other training-associated miRNAs (Fig. S6I).

We therefore went on to evaluate the status of the energy sensor par excellence, AMPK. In this case, *Ampk* showed higher relative expression

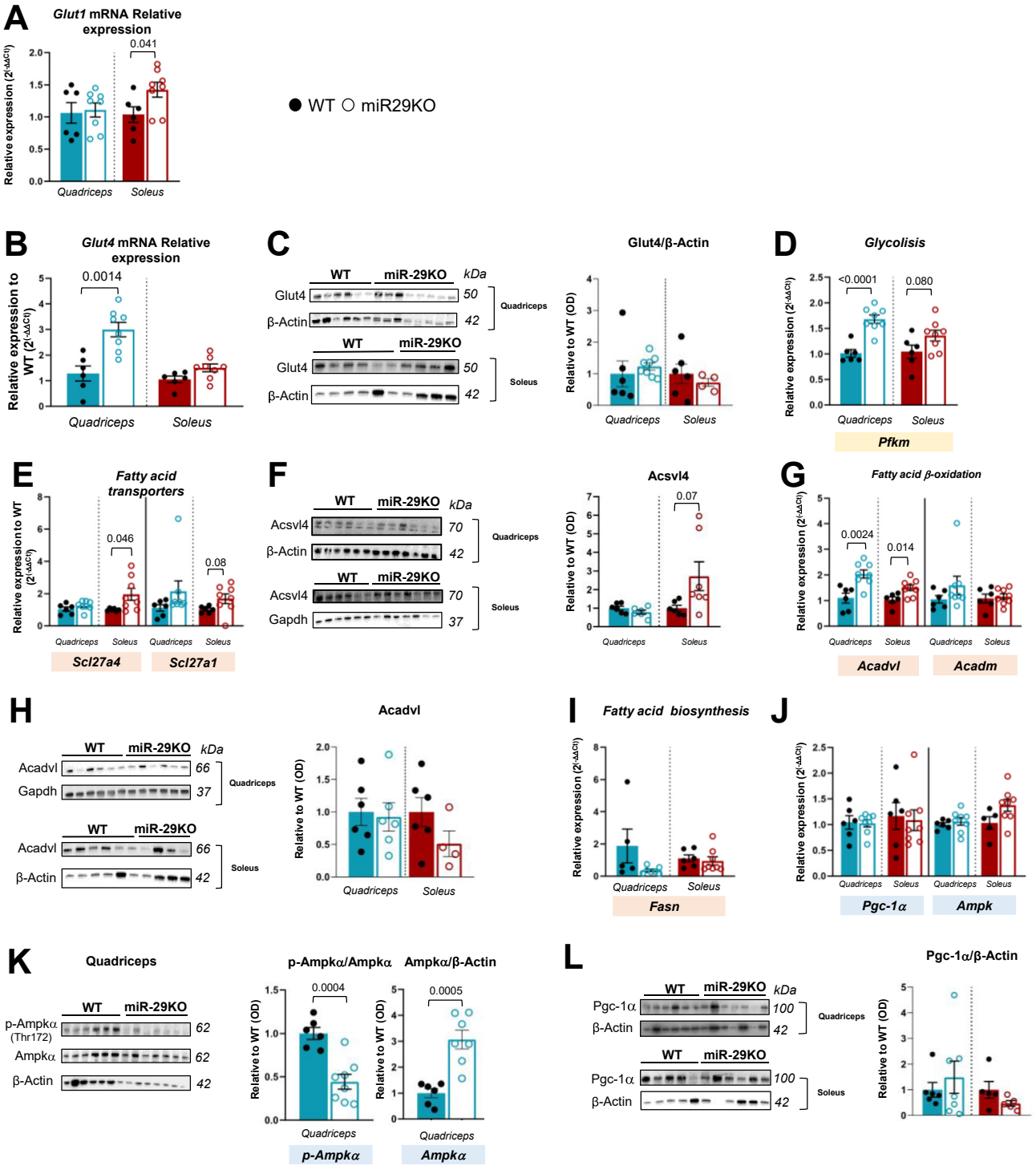

Figure 6: The absence of *miR-29a/b1* increases the availability of energy substrates in quadriceps and soleus but negatively affects their use. A-B. *Glut1* and *Glut4* relative expression in WT and miR-29KO mice. **C.** Analysis of Glut4 protein levels in WT ($n = 6$) and miR-29KO (quadriceps, $n = 8$; soleus, $n = 7$). **D-E.** *Pfkm*, *Slc27a4*, and *Slc27a1* relative expression in WT and miR-29KO mice. **F.** Western blot analysis of Acsvl4 protein in WT ($n = 6$) and miR-29KO mice (quadriceps, $n = 8$; soleus, $n = 7$). **G.** *Acadvl* and *Acadm* relative expression in WT and miR-29KO mice. **H.** Analysis of Acadvl protein levels in WT ($n = 6$) and miR-29KO mice (quadriceps, $n = 6$; soleus, $n = 4$). **I.** *Fasn* relative expression in WT and miR-29KO mice. **J.** *Pgc-1α* and *Ampk* relative expression in WT ($n = 6$) and miR-29KO ($n = 8$) mice. **K.** p-Ampka (Thr^{172}) and total Ampka protein levels in WT ($n = 6$) and miR-29KO mice ($n = 8$). **L.** Western blot analysis of Pgc-1α protein levels in WT (quadriceps, $n = 6$; soleus, $n = 5$) and miR-29KO mice (quadriceps, $n = 7$; soleus, $n = 6$). Statistical significance measured by unpaired, two-tailed Student's *t*-test and *p*-values are indicated in the figures. Data are presented as mean ± SEM. Each dot represents one mouse. If not indicated otherwise, WT ($n = 6$) and miR-29KO ($n = 8$) for both quadriceps and soleus.

levels in the liver of miR-29KO mice (Fig. S6G) and a tendency to increase in soleus, but not in quadriceps (Figure 6J). However, in quadriceps, despite higher total Ampk protein levels, the phosphorylated active form [34] was decreased in miR-29KO mice (Figure 6K), which may indicate a reduced activation of the AMPK pathway.

Given these results, we decided to explore the expression of the *Pgc-1a* gene, one of the main targets of the miR-29 family [13], which is involved in the regulation of both carbohydrate and fatty acid metabolism. Previous research indicated that *Pgc-1a* gene expression was upregulated in the cardiac tissue and liver of miR-29KO mice older than 30-week-old [13]. In contrast, our study revealed no significant differences in *Pgc-1a* mRNA levels in the liver of 16-week-old mice (Fig. S6G), suggesting that liver overexpression might be an age-dependent phenomenon. We did not observe significant alterations in either *Pgc-1a* gene expression or protein levels in both skeletal muscles (Figure 6J,L).

3.6. *miR-29a/b1* cluster deficiency has a profound detrimental effect on the adaptive response to resistance training in skeletal muscle

Since the absence of the *miR-29a/b1* cluster affects both the expression levels of training-associated miRNAs and energy metabolism genes at muscle level, impairing physical capacity, we wanted to study its impact on training adaptation. For this purpose, we used 12-week-old miR-29KO mice and their corresponding WT controls. The initial physical capacity test showed that miR-29KO mice had similar levels of endurance than CON (Figure 7A), while their resistance capacity was significantly lower (Figure 7B). This confirms that the lower resistance capacity observed at 16 weeks (Figure 5C) is already present at 12 weeks in this model.

A 4-week training intervention, analogous to that previously described, was carried out at the same relative intensity. After the training period, endurance-trained miR-29KO mice (miR-29KOEND) improved endurance performance similar to END (Figure 7C). However, resistance-trained mice (miR-29KORES) were only able to maintain their already impaired resistance capacity (Figure 7D), but not improvements in this capacity were observed, contrary to RES. These results reinforce the possible role of *miR-29a/b1* cluster in the adaptive response to resistance training, as we also observed in 16-week-old miR-29KO mice, since it is already present at an early age and worsens over time.

When analyzing the response to training of the training-associated miRNAs, only miR-142a-5p showed lower levels in EVs of miR-29KORES compared to miR-29KO sedentary mice (miR-29KOCON; Figure 7E and Fig. S7A). This miRNA was already described as downregulated in miR-29KOCON compared to CON (Figure 5D).

At muscle level, a different response was observed in miRNA expression between training interventions and between quadriceps and soleus. Thus, resistance training induced a lower expression of let-7i-5p, miR-10b-5p, miR-126a-3p, and miR-143-3p in quadriceps (Figure 7F; Fig. S7B), while in soleus a lower expression of miR-126a-5p was observed, while endurance intervention showed no effect (Figure 7G; Fig. S7C). Therefore, the resistance training intervention partially reversed the miRNA dysregulation observed in quadriceps of miR-29KOCON (Figure 5E), but not in soleus (Figure 5F). As for the liver, although resistance training modified many of the training-associated miRNAs in WT mice (Fig. S8A), no effect was observed in trained miR-29KO mice (Fig. S8B).

Regarding the expression of genes related to energy metabolism, the greatest response was observed to resistance training and the quadriceps was the main responsive tissue (Figure 7H,J, L; Fig. S9), in line with the changes observed in the expression levels of training-associated miRNAs (Figure 7F). Thus, miR-29KORES mice showed lower relative expression levels of *Glut1* and *Glut4* in quadriceps compared to miR-29KOCON mice (Figure 7H). However, Glut4 protein levels were higher in miR-29KORES than in miR-29KOCON (Figure 7I). One possible explanation is that the inducible Glut4 transporter is recycled between stimuli, remaining in a reservoir of cytoplasmic vesicles [35]. Thus, in miR-29KOCON mice, this process could be impaired in the quadriceps. However, resistance training-mediated stimulation could counteract possible deficiencies in either internalization or maintenance and re-exposure of Glut4, thereby reducing the need for increased *Glut4* expression. Similarly, the energy sensor *Ampk* exhibited lower levels of expression in miR-29KORES mice relative to miR-29KOCON (Figure 7J), whereas no changes in total protein levels were observed (Figure 7K). However, the phosphorylated active form was higher in miR-29KORES than miR-29KOCON and miR-29KOEND (Figure 7K). Therefore, it might be possible that resistance training favors the Ampk pathway in the quadriceps of these miR-29KORES mice, enhancing glucose uptake, via Glut4, and its subsequent utilization [35]. An analysis of the fatty acid transporter Acsvl4, at both the expression and protein levels (Figure 7L-M), suggests that improved glucose utilization might reduce the need for a high fatty acid uptake. This contrasts with what was observed in WT mice, where resistance training mainly increased the expression of genes related to fatty acid metabolism in soleus and liver (Fig. S10B—C), similar to what was observed for miRNAs in the liver (Fig. S8A). However, in the quadriceps of WT mice, we did not observe any response to resistance or endurance training (Fig. S10A). That is, resistance training does not restore the miR-29KO phenotype to a metabolic profile more similar to WT mice.

Summarizing, *miR-29a/b1* cluster appears to play a relevant role for the adaptation to resistance training. However, resistance training halts the degeneration of resistance capacity that occurs in the absence of this cluster, suggesting that it could be independent of *miR-29a/b1*. Muscle type-specific repression of other training miRNAs in response to resistance exercise may be mediating this process coupled with prolonged activation of the Ampk/Glut4 axis favoring glucose uptake may be mediating this process.

4. DISCUSSION

One of the mechanisms by which exercise mediates its beneficial effects consists of a systemic crosstalk mediated EVs containing different molecules, including miRNAs [36—38]. However, it remains unresolved the secretory role of skeletal muscle in the response to training as well as which miRNAs encapsulated in EVs might be relevant in this context and contribute to the exercise adaptive process [39]. Traditionally, the characterization of miRNAs contained in EVs in response to acute exercise and training has focused on skeletal muscle-associated miRNAs (myomiRs), such as miR-1, miR-206, and miR-133b (reviewed in [7]). Castaño et al. [27] observed that most plasma EV miRNAs obtained from HIIT-trained mice were myomiRs, proposing skeletal muscle as the main secretory tissue of miRNAs encapsulated in EVs. However, recent research suggests that the presence of myomiRs is higher in interstitial EVs than in plasma EVs, making them more relevant in the context of skeletal muscle regeneration [40].

Thanks to massive sequencing, we have been able to determine that resistance training significantly increases the expression of a group of 11 miRNAs in plasma EVs of mice in response to exercise, with no changes in myomiR expression. However, this does not rule out

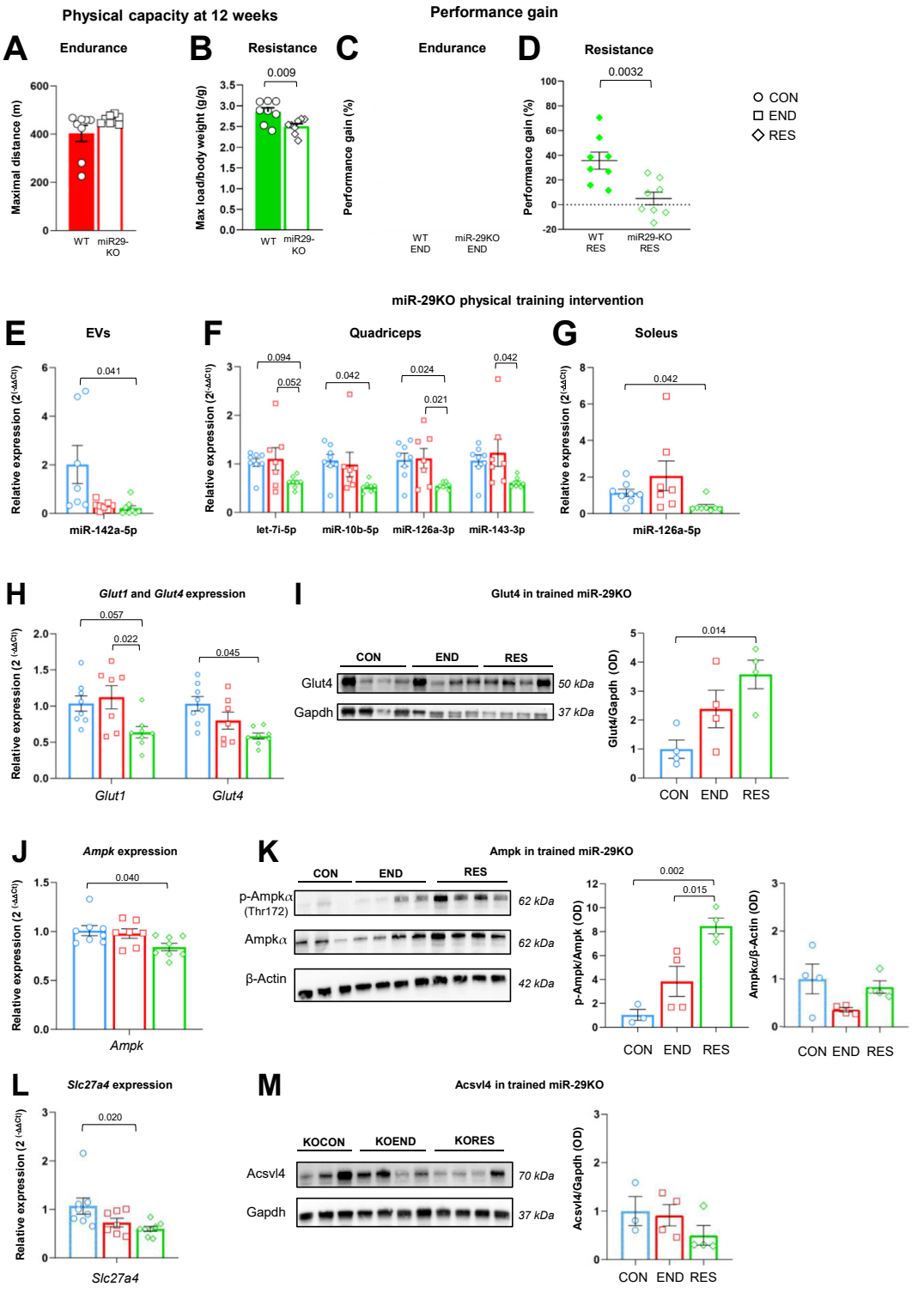

Figure 7: Resistance training exerts an effect on increasing glucose influx and energy production in the quadriceps of miR-29KO mice. A-B. Physical capacity determined as endurance and resistance performance in 12-week WT and miR-29KO mice ($n = 8$). **C-D.** Endurance and resistance performance gain measured as percent variation in WTEND and miR-29KOEND (WTEND, $n = 12$; miR-29KOEND, $n = 8$) and in WTRES and miR-29KORES (WTRES, $n = 8$; miR-29KORES, $n = 8$). Data are presented as percentage mean ± SEM. **E-G.** Effect of exercise intervention in the relative expression levels of training-induced miRNAs, in EVs, quadriceps, and soleus of miR-29KOCON ($n = 8$), miR-29KOEND ($n = 7$), and miR-29KORES ($n = 8$). **H.** *Glut1* and *Glut4* relative expression in control and trained miR-29KO ($n = 4$/group). **I.** Western blot analysis of Glut4 protein levels in control and trained miR-29KO ($n = 4$/group). **J.** *Ampk* relative expression in miR-29KOCON ($n = 8$), miR-29KOEND ($n = 7$), and miR-29KORES ($n = 8$). **K.** Analysis of p-Ampkα (Thr^{172}) and total Ampkα protein levels in miR-29KOCON ($n = 3$), miR-29KOEND ($n = 4$), and miR-29KORES ($n = 4$). **L.** *Slc27a4* relative expression in miR-29KOCON ($n = 8$), miR-29KOEND ($n = 7$), and miR-29KORES ($n = 8$). **M.** Analysis of Acsvl4 protein levels in miR-29KOCON ($n = 3$), miR-29KOEND ($n = 4$), and miR-29KORES ($n = 4$). Statistical analysis was performed by unpaired, two-tailed Student's *t*-test (A–D) and by one-way ANOVA followed by Tuckey's post hoc test (E–M). *p*-values are indicated in the figures. If not indicated otherwise, data are presented as mean ± SEM. Each dot represents one mouse.

skeletal muscle as a secretory tissue for other miRNAs in response to training. In fact, our *in vitro* approaches support that miR-29a-3p and miR-30a-5p are released in EVs in response to skeletal muscle contraction closely resembling the response observed in EVs extracted from the plasma of trained mice. Other authors have also reported the presence of these two miRNAs in EVs in response to an EPS protocol in C2C12 cells and in a more complex three-dimensional model called "myobundles", respectively [41,42]. The involvement of both miRNAs in muscle differentiation and metabolic function is well documented [43—45]. Furthermore, we have observed that the inhibition of miR-29a-3p in cell cultures of myotubes increased the intracellular levels of miR-30a-5p and miR-143-3p, even more so after electrostimulation, yet seems to affect their export in EVs. This could suggest a simultaneous response to the contractile stimulus among various miRNAs from different functional clusters involved in myogenesis and muscle cell differentiation [43—46]. One possible explanation for this could be the role of miR-29a as an epi-miRNA, acting as a connector molecule for various epigenetic mechanisms [47]. In this sense, Rowlands et al. [48] supported the idea that, in response to endurance training, miR-29a downregulation in skeletal muscle in patients with type II diabetes was associated with the epigenetic regulation of the methylation process. Another possible cause is that miR-29a-3p loss may impact the expression of other training-associated miRNAs in skeletal muscle by reducing their binding to Argonaute protein [49] or affecting the biogenesis and secretion of EVs. Interestingly, the *in vitro* model faithfully reflects this coordinated intracellular response, although only in the quadriceps. One possible explanation is that, as described by Abdelmoez et al. [23], this C2C12 cell model showed a higher expression of MYH1 and MYH4 proteins associated with type II fibers, which are more predominant in the quadriceps [50]. However, electrostimulation does not replicate the effect of resistance or endurance training on the intracellular expression of training-associated miRNAs in the muscles tested in miR-29KO mice, and in the case of miR-143-3p the response was the opposite. This difference could be due to the fact that our EPS protocol better reflected the acute response to endurance exercise, based on the frequency and time conditions used [51]. Valero-Bretón et al. [52] reported that replicating the acute and chronic stimulus effect of resistance exercise would have required increasing the stimulation frequency or the number of days, respectively, which was methodologically unfeasible in our model, due to the miR-29a-3p inhibition protocol used.

These results raise the question of whether the increase in miR-29a-3p observed in EVs our *in vivo* model could be due to a prolonged residual effect of the last exercise session, described by Darragh et al. [8] as "last bout effect", rather than the effect of chronic adaptation to training. However, despite limited information in rodent studies, Castaño et al. [27] and Hou et al. [53] described changes in miRNA profile in EVs taken at rest after a period of training. Darragh et al. [39] also proposed that collection of blood samples at least 24 h after cessation of exercise would capture the adaptive response of exerkines to training rather than an acute response. In addition, Whitham et al. [4] reported that, in humans, 4 h after acute exercise EVs concentration returns to basal levels and previous data from our laboratory showed that several of the miRNAs observed in our study, including miR-29a-3p, increased at the circulating level after a marathon in highly trained amateur runners and returned to basal levels 24 h later [54]. Given these findings from both human and murine models, we acknowledge that although the 24-hour post-exercise sampling time may not fully capture all the chronic adaptations associated with sustained training, it remains a relevant time point for assessing molecular responses beyond the immediate acute effects. Therefore, it seems that miR-29a-3p emerges as a molecular mediator released in EVs in response to skeletal muscle contraction, expressed alongside other miRNAs, mainly in response to resistance exercise. Even more, our results show that it could have an important role in the maintenance of physical capacity and for the adaptation to resistance training.

The exacerbated response of genes related to energy substrate availability, both in the muscle and liver tissues, coupled with the drastic reduction of white and brown adipose tissue observed in miR-29KO mice [55—57], seems to be the one of the reasons why these mice adapt to endurance training in a similar way to END. Contrary, miR-29KO mice showed compromised resistance capacity. Specific training did not improve these characteristics, although it prevented maximal strength loss, as we have previously described in a murine model with systemic partial autophagy deficiency [15]. These results emphasize resistance training as an optimal intervention for states of muscular frailty through a variety of underlying molecular mechanisms. Further analysis of this adaptive response to resistance training underlines the importance of miRNA coordinated expression for resistance training adaptation and maximal resistance capacity maintenance. Thus, the repression of let-7i-5p, miR-126a-3p, and miR-143-3p observed in miR-29KORES quadriceps contrasts with the overexpression of these miRNAs in miR-29KOCON. Regarding miR-143-3p, its downregulation after resistance training could be related to increased glucose uptake, mediated by the Glut4 receptor, followed by activation of Ampk for energy production, and contrasted with decreased utilization of lipid metabolism. This prolonged activation of the AMPK/GLUT4 axis could decrease 4E-BP1 phosphorylation [58], a downstream component of mTOR signaling pathway, leading to decreased muscle protein synthesis in these miR-29KORES mice, affecting their adaptation to training. This might suggest that changes in miRNA expression in quadriceps allow this adaptation to resistance training and the maintenance of this capacity, even in the absence of *miR-29a/b1*.

Taken together, this study has defined miR-29a-3p as a novel molecular mediator released in EVs by skeletal muscle in response to contraction stimuli, with an important role in the response and adaptation to resistance training, and mediating a miRNA-driven response in energy metabolism. Additionally, these results suggest that resistance training could be a useful and beneficial intervention for those diseases in which miR-29 family members are downregulated, such as pancreatic and renal fibrosis, osteoporosis [59], and even with a major impact on neurodegeneration [60], as described in Alzheimer's disease [61].

4.1. Limitations

We are aware that our work has several limitations, one of which is that we have only used male mice, which restricts the generalization of our findings. It has been described that sex hormones influence epigenetic responses in the modulation of the EV-miRNA profile after exercise in humans [62]. Furthermore, Lamon et al. [63] described associations between phases of the menstrual cycle, ovarian hormones, and plasma miRNA levels in 20 females with regular menstrual cycle and no record of physical activity habits, which highlights a complex landscape which deserves further deep exploration in future studies. Second, we used a systemic miR-29KO model, which, although it allowed us to investigate the global effects of *miR-29a/b1* deletion, it masks tissue-specific effects. Thus, it would be valuable to conduct future studies using tissue-specific genetic inactivation models, which would offer more detailed insights into the role of miR-29 in specific cellular contexts or the specific secretory activity of different tissues. Additionally, extending the analysis beyond 16 weeks would help uncover any long-term effects of miR-29 deletion. Another

limitation of our study is the use of the Nanodrop assay for protein quantification. Although this method enables the rapid and efficient quantification of a large number of samples, minimizing the amount of tissue used for this purpose, it is less accurate than other methods, such as Bradford or BCA assays, especially in complex lysates. This method was chosen to minimize tissue use, as the amount of available muscle tissues was limited for a wide range of techniques to be performed. However, this may have contributed to variability in protein loading across the gels, potentially affecting the consistency of protein transfer in western blot experiments. Finally, the selection of a 24-hour post-exercise time point presents a limitation in interpreting our findings as purely chronic adaptations. While this time point allows us to assess molecular responses beyond the immediate acute effects, it may not fully capture the long-term adaptations associated with training. In fact, previous studies have shown that acute exercise-induced transcriptional responses in muscle of endurance trained mice peak around 6—8 h post-exercise, but an overlap between acute and long-term transcriptional changes (∼21%) are observed even 18 h after exercise [64]. However, these authors suggest that sustained adaptations are primarily reflected at the proteomic rather than the transcriptomic level [64]. In this sense, Darragh et al. [39] proposed that collecting blood samples at least 24 h post-exercise cessation would capture the adaptive response of exerkines to training, rather than an acute response. Regarding EV and circulating miRNA response to exercise, Whitham et al. [4] found that the EV concentration returns to baseline levels 4 h after exercise, and previous research from our laboratory showed that certain miRNAs, such as miR-29a-3p, increased in circulation after a marathon in highly trained individuals, but returned to baseline levels within 24 h [54]. These results were obtained in humans, since no information about EVs or circulating miRNA dynamics in response to exercise is available in mice. Therefore, future studies incorporating additional time points, including earlier and later post-exercise assessments, would be valuable to better distinguish transient from more persistent molecular responses to exercise in humans and animal models.

ACKNOWLEDGMENTS

We would like to sincerely thank the Scientific-Technical Services of the University of Oviedo for their valuable support. Finally, we would like to thank Javier Bermejo-Pampliega for his work as a research technician at the University of Oviedo, supported by a contract associated with FICYT grant AYUD/2021/5134, confounded by the European Regional Development Fund (ERDF).

CRediT AUTHORSHIP CONTRIBUTION STATEMENT

Paola Pinto-Hernandez: Data curation, Formal analysis, Investigation, Writing — original draft, Writing — review & editing. **Manuel Fernandez-Sanjurjo:** Data curation, Formal analysis, Investigation, Methodology, Supervision, Writing — original draft, Writing — review & editing. **Daan Paget:** Investigation, Writing — review & editing. **Xurde M. Caravia:** Resources, Writing — review & editing. **David Roiz-Valle:** Resources, Writing — review & editing. **Juan Castilla-Silgado:** Investigation, Writing — review & editing. **Sergio Diez-Robles:** Investigation, Writing — review & editing. **Almudena Coto-Vilcapoma:** Investigation, Writing — review & editing. **David Fernandez-Vivero:** Investigation, Writing — review & editing. **Pau Gama-Perez:** Investigation, Writing — review & editing. **Pablo M. Garcia-Roves:** Investigation, Writing — review & editing. **Carlos Lopez-Otin:** Resources, Writing — review & editing. **Juleen R. Zierath:** Resources, Writing — review & editing. **Anna Krook:** Resources, Writing — review & editing. **Benjamin Fernandez-Garcia:** Conceptualization, Funding acquisition, Investigation, Project administration, Supervision, Writing — original draft, Writing — review & editing. **Cristina Tomas-Zapico:** Conceptualization, Funding acquisition, Investigation, Supervision, Writing — original draft, Writing — review & editing. **Eduardo Iglesias-Gutierrez:** Conceptualization, Funding acquisition, Investigation, Methodology, Project administration, Supervision, Writing — original draft, Writing — review & editing.

DECLARATION OF COMPETING INTEREST

The authors declare that they have no known competing financial interests or personal relationships that could have appeared to influence the work reported in this paper.

FUNDING

P.P—H. was supported by a contract associated with grant AYUD/2021/5134 from FICYT (Plan de Ciencia, Tecnología e Innovación 2018—2022 del Principado de Asturias), cofunded by the Fondo Europeo de Desarrollo Regional (FEDER), Spain. J.C.-S. was supported by a contract associated with grant AC20/00017 from Instituto de Salud Carlos III, Spain, cofounded by EuroNanoMed III (grant 20-0084). A.C.-V. was supported by a contract associated with grant AYUD/2021/57540 from FICYT/FEDER, Spain.
This work was supported by the Fundación Tatiana Pérez de Guzmán el Bueno (Convocatoria de ayudas a proyectos de investigación en neurociencia, edición 2020) to C.T.-Z. and E.I.-G and by the Spanish Ministerio de Economía y Competitividad (DEP2012-39262 and DEP2015-69980-P) to EI-G and BF-G.

DATA AVAILABILITY

Data will be made available on request.

DATA AND CODE AVAILABILITY

Raw RNA-Seq data have been deposited at Zenodo and are publicly accessible as of the date of publication. Accession link is listed in the key resources table.
All the values used to create graphs in the paper can be found in the Data Main Figures file in a single Excel spreadsheet.
The raw uncropped western blots can be found in the Data Supplemental Figures file in a single PDF document.
Additional information required to reanalyze the data reported in this paper is available from the lead contact upon request.

APPENDIX A. SUPPLEMENTARY DATA

Supplementary data to this article can be found online at https://doi.org/10.1016/j.molmet.2025.102173.

REFERENCES

[1] Thompson WR, Sallis R, Joy E, Jaworski CA, Stuhr RM, Trilk JL. Exercise is medicine. Am J Lifestyle Med 2020;14(5):511—23.
[2] Safdar A, Saleem A, Tarnopolsky MA. The potential of endurance exercise-derived exosomes to treat metabolic diseases. Nat Rev Endocrinol 2016;12(9):504—17.

[3] Brahmer A, Neuberger E, Esch-Heisser L, Haller N, Jorgensen MM, Baek R, et al. Platelets, endothelial cells and leukocytes contribute to the exercise-triggered release of extracellular vesicles into the circulation. J Extracell Vesicles 2019;8(1):1615820.
[4] Whitham M, Parker BL, Friedrichsen M, Hingst JR, Hjorth M, Hughes WE, et al. Extracellular vesicles provide a means for tissue crosstalk during exercise. Cell Metab 2018;27(1):237—251 e234.
[5] Abels ER, Breakefield XO. Introduction to extracellular vesicles: biogenesis, RNA cargo selection, content, release, and uptake. Cell Mol Neurobiol 2016;36(3):301—12.
[6] O'Brien K, Breyne K, Ughetto S, Laurent LC, Breakefield XO. RNA delivery by extracellular vesicles in Mammalian cells and its applications. Nat Rev Mol Cell Biol 2020;21(10):585—606.
[7] Estebanez B, Jimenez-Pavon D, Huang CJ, Cuevas MJ, Gonzalez-Gallego J. Effects of exercise on exosome release and cargo in *in vivo* and ex vivo models: a systematic review. J Cell Physiol 2021;236(5):3336—53.
[8] Darragh IAJ, O'Driscoll L, Egan B. Exercise training and circulating small extracellular vesicles: appraisal of methodological approaches and current knowledge. Front Physiol 2021;12:738333.
[9] Isaac R, Reis FCG, Ying W, Olefsky JM. Exosomes as mediators of intercellular crosstalk in metabolism. Cell Metab 2021;33(9):1744—62.
[10] Ebert MS, Sharp PA. Roles for microRNAs in conferring robustness to biological processes. Cell 2012;149(3):515—24.
[11] Yanez-Mo M, Siljander PR, Andreu Z, Zavec AB, Borras FE, Buzas EI, et al. Biological properties of extracellular vesicles and their physiological functions. J Extracell Vesicles 2015;4:27066.
[12] Murphy RM, Watt MJ, Febbraio MA. Metabolic communication during exercise. Nat Metab 2020;2(9):805—16.
[13] Caravia XM, Fanjul V, Oliver E, Roiz-Valle D, Moran-Alvarez A, Desdin-Mico G, et al. The microRNA-29/PGC1alpha regulatory axis is critical for metabolic control of cardiac function. PLoS Biol 2018;16(10):e2006247.
[14] Iglesias-Gutierrez E, Fernandez-Sanjurjo M, Fernandez AF, Rodriguez Diaz FJ, Lopez-Taboada I, Tomas-Zapico C, et al. Versatility of protocols for resistance training and assessment using static and dynamic ladders in animal models. J Vis Exp 2021;178.
[15] Codina-Martinez H, Fernandez-Garcia B, Diez-Planelles C, Fernandez AF, Higarza SG, Fernandez-Sanjurjo M, et al. Autophagy is required for performance adaptive response to resistance training and exercise-induced adult neurogenesis. Scand J Med Sci Sports 2020;30(2):238—53.
[16] Fernandez J, Fernandez-Sanjurjo M, Iglesias-Gutierrez E, Martinez-Camblor P, Villar CJ, Tomas-Zapico C, et al. Resistance and endurance exercise training induce differential changes in gut microbiota composition in murine models. Front Physiol 2021;12:748854.
[17] Kemi OJ, Loennechen JP, Wisloff U, Ellingsen O. Intensity-controlled treadmill running in mice: cardiac and skeletal muscle hypertrophy. J Appl Physiol 2002;93(4):1301—9.
[18] Figueiredo VC, de Salles BF, Trajano GS. Volume for muscle hypertrophy and health outcomes: the Most effective variable in resistance training. Sports Med 2018;48(3):499—505.
[19] Gentil P, Marques VA, Neto JPP, Santos ACG, Steele J, Fisher J, et al. Using velocity loss for monitoring resistance training effort in a real-world setting. Appl Physiol Nutr Metabol 2018;43(8):833—7.
[20] Invalid citation !!! [vol. 20].
[21] Vlachos IS, Paraskevopoulou MD, Karagkouni D, Georgakilas G, Vergoulis T, Kanellos I, et al. DIANA-TarBase v7.0: indexing more than half a million experimentally supported miRNA:mRNA interactions. Nucleic Acids Res 2015;43(Database issue):D153—9.
[22] Vlachos IS, Zagganas K, Paraskevopoulou MD, Georgakilas G, Karagkouni D, Vergoulis T, et al. DIANA-miRPath v3.0: deciphering microRNA function with experimental support. Nucleic Acids Res 2015;43(W1):W460—6.
[23] Abdelmoez AM, Sardon Puig L, Smith JAB, Gabriel BM, Savikj M, Dollet L, et al. Comparative profiling of skeletal muscle models reveals heterogeneity of transcriptome and metabolism. Am J Physiol Cell Physiol 2020;318(3):C615—26.
[24] Mestdagh P, Hartmann N, Baeriswyl L, Andreasen D, Bernard N, Chen C, et al. Evaluation of quantitative miRNA expression platforms in the microRNA quality control (miRQC) study. Nat Methods 2014;11(8):809—15.
[25] Livak KJ, Schmittgen TD. Analysis of relative gene expression data using real-time quantitative PCR and the 2(-Delta Delta C(T)) method. Methods 2001;25(4):402—8.
[26] Mestdagh P, Van Vlierberghe P, De Weer A, Muth D, Westermann F, Speleman F, et al. A novel and universal method for microRNA RT-qPCR data normalization. Genome Biol 2009;10(6):R64.
[27] Castano C, Mirasierra M, Vallejo M, Novials A, Parrizas M. Delivery of muscle-derived exosomal miRNAs induced by HIIT improves insulin sensitivity through down-regulation of hepatic FoxO1 in mice. Proc Natl Acad Sci U S A 2020;117(48):30335—43.
[28] Paola Pinto-Hernandez MF-S, Iglesias-Gutierrez Eduardo, Fernandez-Garcia Benjamin. miR-29a-3p, a new myokine orchestrating resistance exercise via coordinated metabolic responses Zenodo. 2024.
[29] Dastah S, Tofighi A, Bonab SB. The effect of aerobic exercise on the expression of mir-126 and related target genes in the endothelial tissue of the cardiac muscle of diabetic rats. Microvasc Res 2021;138:104212.
[30] Rubenstein AB, Smith GR, Raue U, Begue G, Minchev K, Ruf-Zamojski F, et al. Single-cell transcriptional profiles in human skeletal muscle. Sci Rep 2020;10(1):229.
[31] Kavakiotis I, Alexiou A, Tastsoglou S, Vlachos IS, Hatzigeorgiou AG. DIANA-miTED: a microRNA tissue expression database. Nucleic Acids Res 2022;50(D1):D1055—61.
[32] Kriegel AJ, Liu Y, Fang Y, Ding X, Liang M. The miR-29 family: genomics, cell biology, and relevance to renal and cardiovascular injury. Physiol Genom 2012;44(4):237—44.
[33] Ferreira JC, Rolim NP, Bartholomeu JB, Gobatto CA, Kokubun E, Brum PC. Maximal lactate steady state in running mice: effect of exercise training. Clin Exp Pharmacol Physiol 2007;34(8):760—5.
[34] Willows R, Sanders MJ, Xiao B, Patel BR, Martin SR, Read J, et al. Phosphorylation of AMPK by upstream kinases is required for activity in Mammalian cells. Biochem J 2017;474(17):3059—73.
[35] Richter EA, Hargreaves M. Exercise, GLUT4, and skeletal muscle glucose uptake. Physiol Rev 2013;93(3):993—1017.
[36] Guo L, Quan M, Pang W, Yin Y, Li F. Cytokines and exosomal miRNAs in skeletal muscle-adipose crosstalk. Trends Endocrinol Metabol 2023;34(10):666—81.
[37] Ni P, Yang L, Li F. Exercise-derived skeletal myogenic exosomes as mediators of intercellular crosstalk: a major player in health, disease, and exercise. J Physiol Biochem 2023;79(3):501—10.
[38] Fischetti F, Poli L, De Tommaso M, Paolicelli D, Greco G, Cataldi S. The role of exercise parameters on small extracellular vesicles and microRNAs cargo in preventing neurodegenerative diseases. Front Physiol 2023;14:1241010.
[39] Darragh IAJ, Egan B. Considerations for exerkine research focusing on the response to exercise training. J Sport Health Sci 2024;13(2):130—2.
[40] Watanabe S, Sudo Y, Makino T, Kimura S, Tomita K, Noguchi M, et al. Skeletal muscle releases extracellular vesicles with distinct protein and microRNA signatures that function in the muscle microenvironment. PNAS Nexus 2022;1(4):pgac173.
[41] Lautaoja-Kivipelto JH, Karvinen S, Korhonen TM, O'Connell TM, Tiirola M, Hulmi JJ, et al. Interaction of the C2C12 myotube contractions and glucose availability on transcriptome and extracellular vesicle microRNAs. Am J Physiol Cell Physiol 2024;326(2):C348—61.
[42] Vann CG, Zhang X, Khodabukus A, Orenduff MC, Chen YH, Corcoran DL, et al. Differential microRNA profiles of intramuscular and secreted extracellular vesicles in human tissue-engineered muscle. Front Physiol 2022;13:937899.

[43] Soriano-Arroquia A, McCormick R, Molloy AP, McArdle A, Goljanek-Whysall K. Age-related changes in miR-143-3p:Igfbp5 interactions affect muscle regeneration. Aging Cell 2016;15(2):361–9.
[44] Guess MG, Barthel KK, Harrison BC, Leinwand LA. miR-30 family microRNAs regulate myogenic differentiation and provide negative feedback on the microRNA pathway. PLoS One 2015;10(2):e0118229.
[45] Wei W, He HB, Zhang WY, Zhang HX, Bai JB, Liu HZ, et al. miR-29 targets Akt3 to reduce proliferation and facilitate differentiation of myoblasts in skeletal muscle development. Cell Death Dis 2013;4(6):e668.
[46] Du J, Zhang Y, Shen L, Luo J, Lei H, Zhang P, et al. Effect of miR-143-3p on C2C12 myoblast differentiation. Biosci Biotechnol Biochem 2016;80(4):706–11.
[47] Fabbri M, Garzon R, Cimmino A, Liu Z, Zanesi N, Callegari E, et al. MicroRNA-29 family reverts aberrant methylation in lung cancer by targeting DNA methyltransferases 3A and 3B. Proc Natl Acad Sci U S A 2007;104(40):15805–10.
[48] Rowlands DS, Page RA, Sukala WR, Giri M, Ghimbovschi SD, Hayat I, et al. Multi-omic integrated networks connect DNA methylation and miRNA with skeletal muscle plasticity to chronic exercise in type 2 diabetic obesity. Physiol Genom 2014;46(20):747–65.
[49] Luna JM, Barajas JM, Teng KY, Sun HL, Moore MJ, Rice CM, et al. Argonaute CLIP defines a deregulated miR-122-Bound transcriptome that correlates with patient survival in human liver cancer. Mol Cell 2017;67(3):400–410 e407.
[50] Schiaffino S, Reggiani C. Fiber types in Mammalian skeletal muscles. Physiol Rev 2011;91(4):1447–531.
[51] Nikolic N, Bakke SS, Kase ET, Rudberg I, Flo Halle I, Rustan AC, et al. Electrical pulse stimulation of cultured human skeletal muscle cells as an *in vitro* model of exercise. PLoS One 2012;7(3):e33203.
[52] Valero-Breton M, Warnier G, Castro-Sepulveda M, Deldicque L, Zbinden-Foncea H. Acute and chronic effects of high frequency electric pulse stimulation on the Akt/mTOR pathway in human primary myotubes. Front Bioeng Biotechnol 2020;8:565679.
[53] Hou Z, Qin X, Hu Y, Zhang X, Li G, Wu J, et al. Longterm exercise-derived exosomal miR-342-5p: a novel exerkine for cardioprotection. Circ Res 2019;124(9):1386–400.
[54] de Gonzalo-Calvo D, Davalos A, Fernandez-Sanjurjo M, Amado-Rodriguez L, Diaz-Coto S, Tomas-Zapico C, et al. Circulating microRNAs as emerging cardiac biomarkers responsive to acute exercise. Int J Cardiol 2018;264:130–6.
[55] Song H, Ding L, Zhang S, Wang W. MiR-29 family members interact with SPARC to regulate glucose metabolism. Biochem Biophys Res Commun 2018;497(2):667–74.
[56] Esteves JV, Enguita FJ, Machado UF. MicroRNAs-Mediated regulation of skeletal muscle GLUT4 expression and translocation in insulin resistance. J Diabetes Res 2017;2017:7267910.
[57] Massart J, Sjogren RJO, Lundell LS, Mudry JM, Franck N, O'Gorman DJ, et al. Altered miR-29 expression in type 2 diabetes influences glucose and lipid metabolism in skeletal muscle. Diabetes 2017;66(7):1807–18.
[58] Dreyer HC, Fujita S, Cadenas JG, Chinkes DL, Volpi E, Rasmussen BB. Resistance exercise increases AMPK activity and reduces 4E-BP1 phosphorylation and protein synthesis in human skeletal muscle. J Physiol 2006;576(Pt 2):613–24.
[59] Horita M, Farquharson C, Stephen LA. The role of miR-29 family in disease. J Cell Biochem 2021;122(7):696–715.
[60] Roshan R, Shridhar S, Sarangdhar MA, Banik A, Chawla M, Garg M, et al. Brain-specific knockdown of miR-29 results in neuronal cell death and ataxia in mice. RNA 2014;20(8):1287–97.
[61] Hebert SS, Horre K, Nicolai L, Papadopoulou AS, Mandemakers W, Silahtaroglu AN, et al. Loss of microRNA cluster miR-29a/b-1 in sporadic Alzheimer's disease correlates with increased BACE1/beta-secretase expression. Proc Natl Acad Sci U S A 2008;105(17):6415–20.
[62] Kargl CK, Sterczala AJ, Santucci D, Conkright WR, Krajewski KT, Martin BJ, et al. Circulating extracellular vesicle characteristics differ between men and women following 12 weeks of concurrent exercise training. Phys Rep 2024;12(9):e16016.
[63] Lamon S, Le Carre J, Petito G, Duong HP, Luthi F, Hiam D, et al. The effect of the menstrual cycle on the circulating microRNA pool in human plasma: a pilot study. Hum Reprod 2023;38(1):46–56.
[64] Furrer R, Heim B, Schmid S, Dilbaz S, Adak V, Nordstrom KJV, et al. Molecular control of endurance training adaptation in Male mouse skeletal muscle. Nat Metab 2023;5(11):2020–35.

